EVOLUTIONARY BIOLOGY

Speciation dynamics and extent of parallel evolution along a lake-stream environmental contrast in African cichlid fishes

Alexandra A.-T. Weber*†‡, Jelena Rajkov§, Kolja Smailus, Bernd Egger, Walter Salzburger*

Understanding the dynamics of speciation is a central topic in evolutionary biology. Here, we investigated how morphological and genomic differentiation accumulated along the speciation continuum in the African cichlid fish *Astatotilapia burtoni*. While morphological differentiation was continuously distributed across different lake-stream population pairs, we found that there were two categories with respect to genomic differentiation, suggesting a "gray zone" of speciation at ~0.1% net nucleotide divergence. Genomic differentiation was increased in the presence of divergent selection and drift compared to drift alone. The quantification of phenotypic and genetic parallelism in four cichlid species occurring along a lake-stream environmental contrast revealed parallel and antiparallel components in rapid adaptive divergence, and morphological convergence in species replicates inhabiting the same environments. Furthermore, we show that the extent of parallelism was higher when ancestral populations were more similar. Our study highlights the complementary roles of divergent selection and drift on speciation and parallel evolution.

INTRODUCTION

The formation of new species, speciation, is a fundamental evolutionary process that has attracted much interest during the past 160 years (*1*–*3*). However, relatively little is known about how genomic and morphological differentiation accumulates along the so-called speciation continuum (*4*). The dynamics of genomic differentiation associated with the divergence of populations has previously been explored using modeling (*5*), empirical data (*6*–*8*), or a combination of both (*9*), revealing examples for both scenarios, the "sudden" transition from a state of well-intermixed populations to two reproductively isolated entities (*5*, *6*) and the more gradual accumulation of genomic divergence (*7*, *8*). In contrast, the dynamics of morphological diversification has only rarely been assessed in the context of the speciation continuum. Likewise, only few study systems have been established that allow joint investigation of early and late stages of genomic and morphological differentiation along the entire speciation continuum. Inferring these differentiation trajectories is crucial, however, to understand the underlying processes and, possibly, to identify thresholds of differentiation that delimit species boundaries.

The integrative examination of morphological and genomic differentiation also allows the evaluation of whether the speciation process is predictable (*10*, *11*), for example, by examining evolutionary parallelism at the level of phenotypes and of genotypes across population pairs diverging along similar environmental contrasts (*11*). In fishes, it appears that adaptive divergence involves both parallel and nonparallel components, that is, while some traits or genes were found to evolve in parallel, others in different systems did not [reviewed in (*12*)]. Recently, the concept of (non-)parallel evolution has been introduced as a gradient ranging from truly parallel to completely divergent evolution (*13*). This concept also allows for a better quantification of the extent of parallelism and to distinguish between convergence and parallelism, whereby in convergent evolution, similar types evolve from different ancestral states, whereas in parallel evolution, the starting points are similar (*13*). In general, it is assumed that the extent of parallelism becomes smaller the more distantly related two populations are, which is likely due to reduced levels of shared genetic variation in these populations (*11*). Empirical work in threespine stickleback fish that repeatedly colonized freshwater habitats from marine environments supports this view (*14*, *15*). However, to the best of our knowledge, the extent of parallelism as a function of relatedness has not yet been quantified across a continuum of genomic divergence spanning from closely related populations to different species that diverged along a similar environmental contrast.

Here, we investigate differentiation trajectories and the extent of parallel evolution in East African cichlid fishes, which constitute important model taxa in speciation research and serve as textbook examples of adaptive radiations characterized by rapid speciation accompanied by the evolution of substantial phenotypic, behavioral, and ecological diversity (*16*–*18*). More specifically, we examine the dynamics of morphological and genomic diversification along a lake-stream environmental contrast in the East African cichlid fish *Astatotilapia burtoni* (Günther, 1893) across its native distribution range. *A. burtoni*, which occurs in African Lake Tanganyika and affluent rivers (Fig. 1A), was among the first five cichlid species to have their genomes sequenced (*19*). It is a generalist able to feed on a variety of food sources and can thrive in varied environments such as rivers and lakes (*20*), thus representing an ideal model to investigate the dynamics of diversification along an environmental contrast across different temporal and geographic scales. Lake Tanganyika is the oldest African Great Lake (~10 million years old) and has a complex paleoenvironmental history characterized by, for example, substantial lake-level fluctuations caused by variations in rainfall regimes, temperature, evaporation, and tectonic activity

Zoological Institute, Department of Environmental Sciences, University of Basel, Basel, Switzerland.
*Corresponding author. Email: ale.weber@unibas.ch (A.A.-T.W.); walter.salzburger@unibas.ch (W.S.)
†Present address: Sciences, Museums Victoria, Melbourne, Victoria, Australia.
‡Present address: Laboratoire Environnement Profond, Centre de Bretagne, REM/EEP, Ifremer, Plouzané, France.
§Present address: Marine Evolutionary Ecology, GEOMAR-Helmholtz Centre for Ocean Research, Kiel, Germany.

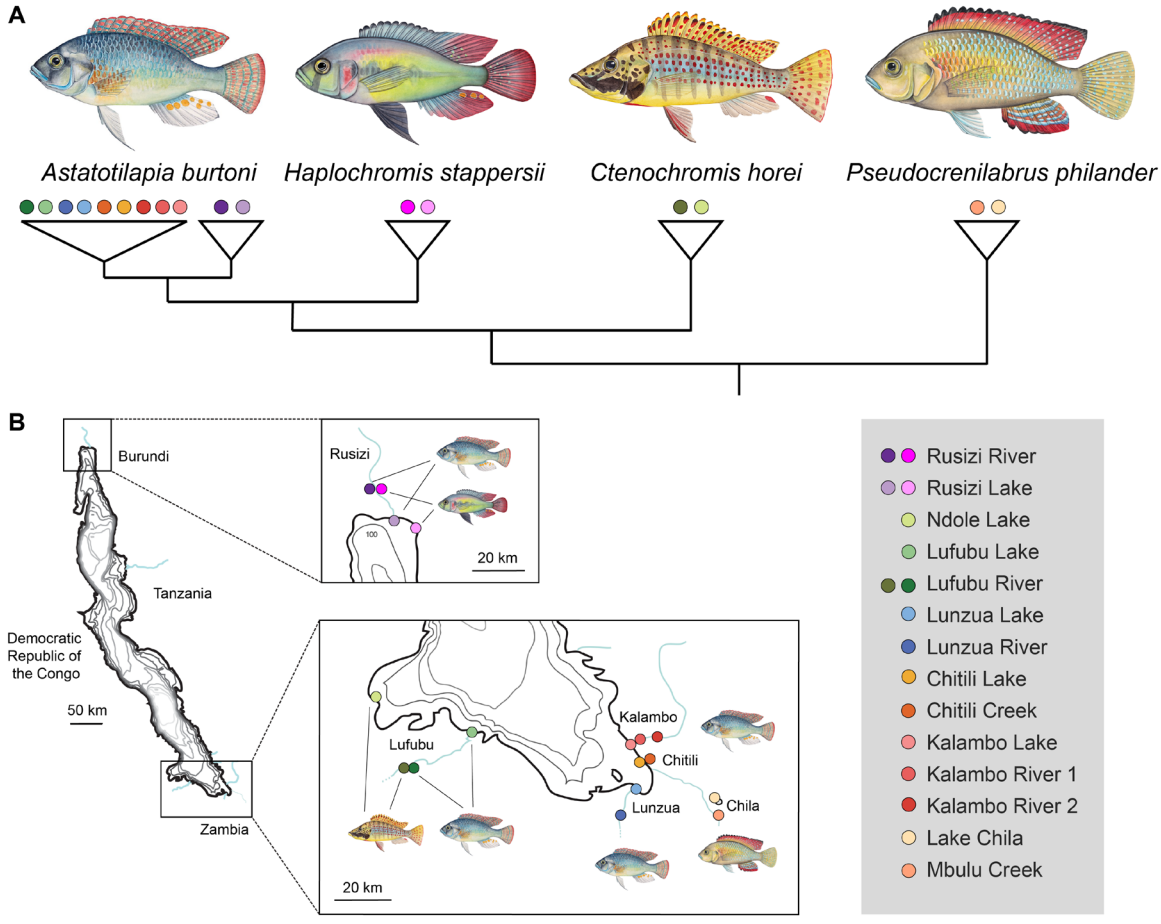

Fig. 1. The study system comprising nine lake-stream population pairs in four cichlid fish species from African Lake Tanganyika and surroundings. (**A**) Illustrations of the four species used in this study and a schematic representation of their phylogenetic relationships [see fig. S1 and (*18*) for details]. (**B**) Map of sampling localities and names of the different lake-stream population pairs, that is, systems. *A. burtoni* ($n_{genomes}$ = 132; $n_{morphometrics}$ = 289), *C. horei* ($n_{genomes}$ = 24; $n_{morphometrics}$ = 67), *H. stappersii* ($n_{genomes}$ = 24; $n_{morphometrics}$ = 81), and *P. philander* ($n_{genomes}$ = 24; $n_{morphometrics}$ = 31).

(*21*, *22*). In particular, lake-level lowstands during arid phases are likely to also have affected the tributaries of Lake Tanganyika and the locations of their estuaries into the main lake. Many of these tributaries, be they small creeks or larger rivers, are inhabited by *A. burtoni* populations derived from lake fish, thereby forming "population pairs" consisting of a source (that is, ancestral) population in the lake and a phenotypically distinct river population featuring habitat-specific adaptations in morphology and ecology (*20*, *23*). For example, stream fish have a more inferior mouth position and a more slender body than lake fish (*20*). The different population pairs display varying levels of genomic differentiation, ranging from virtually no divergence to highly differentiated populations, and show strong signals of isolation by distance (*23*). A comprehensive phylogeographic study of *A. burtoni* across Lake Tanganyika revealed that the populations from the North and the South of Lake Tanganyika are genetically clearly distinct (*24*).

To quantify the extent of parallel evolution in lake-stream divergence not only within species but also between species co-occurring in the same river systems, we further examined lake-stream population pairs of three additional cichlid species (*18*), namely, *Ctenochromis horei*, *Haplochromis stappersii*, and *Pseudocrenilabrus philander* (Fig. 1A) [the taxonomy follows (*25*)]. Two of these species co-occur in sympatry with *A. burtoni* in two of the largest tributaries to Lake Tanganyika (*C. horei* in the Lufubu River in the South and *H. stappersii* in the Rusizi River in the North), providing an excellent opportunity to examine two species replicates of lake-stream divergence in the very same river systems. We used whole-genome resequencing, geometric morphometric analyses, and mate-choice experiments to (i) assess the dynamics of morphological and genomic differentiation along the lake-stream environmental contrast and across geography in *A. burtoni*, (ii) evaluate to what extent genome-wide differentiation scales with reproductive isolation in *A. burtoni*, (iii) quantify the extent of morphological and genomic parallelism and convergence among nine lake-stream population pairs from four cichlid species, and (iv) test whether the extent of parallelism is higher when ancestral (i.e., lake) populations are more similar.

RESULTS

We performed whole-genome resequencing of 180 specimens of cichlid fishes from Lake Tanganyika and its surroundings (132 *A. burtoni* and 24 of each of *C. horei* and *H. stappersii*) and included available sequence data of 24 individuals of *P. philander* (*26*). We

examined six *A. burtoni* lake-stream population pairs and one population pair for each of the three additional species (*C. horei*, *H. stappersii*, and *P. philander*), totaling nine lake-stream population pairs (see Materials and Methods, Fig. 1, fig. S1, and tables S1 and S2). Each population pair consisted of one lake and one stream population, whereby the lake population was sampled from a lake habitat close to the stream's estuary. The population pairs, or "systems," were named after the respective river, except for the Lake Chila system (Fig. 1B). Note that from the Kalambo drainage, we sampled two ecologically distinct riverine populations, one from a locality near the estuary where the river is deep and flows slowly (Kalambo 1) and the other one from about 6-km upstream in a white-water environment (Kalambo 2), resulting in two population pairs for this system (*20*). In addition, we quantified body shape of 468 specimens covering all 17 populations (table S2). Last, we evaluated the degree of reproductive isolation between *A. burtoni* populations displaying increasing levels of genomic divergence. To do so, we revisited published studies that examined the same *A. burtoni* populations as in the present study and, in addition, performed mate-choice experiments in the laboratory between the genetically most distinct *A. burtoni* populations from the North and the South of Lake Tanganyika.

The dynamics of morphological and genomic diversification

We first compared morphological [Mahalanobis distance (D_M)] and genomic (genome-wide F_{ST}) differentiation across all 11 *A. burtoni* populations to examine the respective roles of environmental variation and geography in diversification, classifying the 55 pairwise comparisons according to habitat contrasts (lake-lake, lake-stream, and stream-stream) and to the geographic distance between populations (1 to 40 km, South-East of Lake Tanganyika; 70 to 140 km, East-West; and 700 to 750 km, North-South; see Fig. 1B). The analysis of body shape revealed that all populations differed significantly from one another in average body shape (table S3). The distribution of pairwise D_M values, which ranged from 2.1 (Lunzua lake versus Kalambo lake) to 7.6 (Rusizi lake versus Lufubu River), was continuous (Fig. 2A and table S3). In all three geographic groups (South-East, East-West, and North-South), the most similar system pairs according to pairwise D_M values were lake-lake comparisons (i.e., populations from similar environments), whereas the most distinct ones were lake-stream comparisons (i.e., populations from different environments), suggesting that ecological factors affect body shape differentiation. Last, a wide range of D_M values was observed within a small geographic range (1 to 40 km: Lunzua lake versus Kalambo lake, $D_M = 2.1$; Chitili River versus Kalambo lake, $D_M = 6.3$), suggesting that body shape can differ substantially across small geographic distances and at low levels of genome-wide divergence (Fig. 2A and fig. S2).

Contrary to morphological differentiation, we observed a sudden increase in the levels of genomic differentiation between population pairs, with two clearly separated categories in the pairwise F_{ST} values (≤ 0.3 and ≥ 0.6), hereafter referred to as the "one-species category" and the "two-species category," respectively (Fig. 2B). All pairwise comparisons between the South-East populations and between any of the South-East populations and the Lufubu lake population were assigned into the one-species category, just as the comparison between the two Rusizi populations. The two-species category included all pairwise comparisons between any of the South-East populations and the Lufubu River population and all comparisons involving one southern and one northern population. From this, it emerges that geographic distance alone is not sufficient to explain the extent of genetic divergence, as, for example, pairwise comparisons of populations with moderate geographic distances (70 to 140 km) were found in both F_{ST} categories. Instead, it appears that the separation at moderate geographic distance was driven by both adaptation to different habitats and genetic drift (see also below). We found a single pairwise comparison showing an F_{ST} value in between the one-species and the two-species categories, namely, the population pair from the Lufubu system (Lufubu lake versus Lufubu River: $F_{ST} = 0.46$). Demographic modeling of this population pair indicated that the most likely scenario of divergence between these populations involved a past secondary contact event, that is, one or several periods of allopatric divergence in the past with currently ongoing gene flow (fig. S3 and table S4).

Next, we investigated the increase in genomic differentiation against a proxy of time since population divergence, net nucleotide difference [$D_a = d_{XY} - ((\pi_1 + \pi_2)/2)$]. To extend the comparative framework to encompass the entire continuum of genomic divergence from populations to species, we included the between-species comparisons of the three additional species *C. horei*, *H. stappersii*, and *P. philander*. We found a rapid increase in F_{ST} at low levels of D_a, which slowed down as D_a increased. Given this trend, we fitted a logarithmic model to the data, which was highly significant [linear regression $F_{ST} \sim \log(D_a)$, $P < 2.2 \times 10^{-16}$; Pearson correlation coefficient, $R^2 = 0.96$]. Therefore, to better visualize the dynamics of diversification at early stages of genomic differentiation, we plotted D_a on a logarithmic scale (Fig. 2B). The one-species category encompassed D_a values ranging from 5×10^{-6} to 5×10^{-4}, while the two-species category features D_a values of 0.002 and above. With $D_a \sim 0.001$, the population pair from the Lufubu system occupied the "gray zone" of speciation between the one-species and two-species categories.

Reproductive isolation begins establishing at low levels of genome-wide differentiation

As a next step, we assessed to what extent the observed levels of genome-wide differentiation scale with the degree of reproductive isolation between populations in *A. burtoni*. To this end, we revisited available data from previous experiments that used the same *A. burtoni* populations as in the present study (*20*, *27*, *28*) and conducted additional mate-choice experiments in the laboratory between the genetically most distinct populations of *A. burtoni* from the North and the South of Lake Tanganyika (Table 1, Supplementary Text, and fig. S4) (*24*).

Previous experiments involving populations that feature low levels of genomic divergence [Kalambo lake versus Kalambo River 2, $F_{ST} = 0.11$ (*27*); Kalambo lake versus Lunzua River, $F_{ST} = 0.12$ (*20*)] revealed random mating patterns with respect to source population, suggesting a lack of reproductive isolation. In a mesocosm experiment in a seminatural setting at Lake Tanganyika with populations at a slightly higher level of genome-wide differentiation, yet still within the one-species category (Kalambo lake versus Ndole lake, $F_{ST} = 0.18$), a weak signal of extrinsic hybrid inviability was detected (*28*). In contrast, populations at intermediate (Ndole lake versus Lufubu River, $F_{ST} = 0.47$) and high (Kalambo lake versus Lufubu River, $F_{ST} = 0.62$) levels of genome-wide divergence showed strong signs of extrinsic hybrid inviability in the same mesocosm experiment (*28*). Notably, these differences in the extent of reproductive

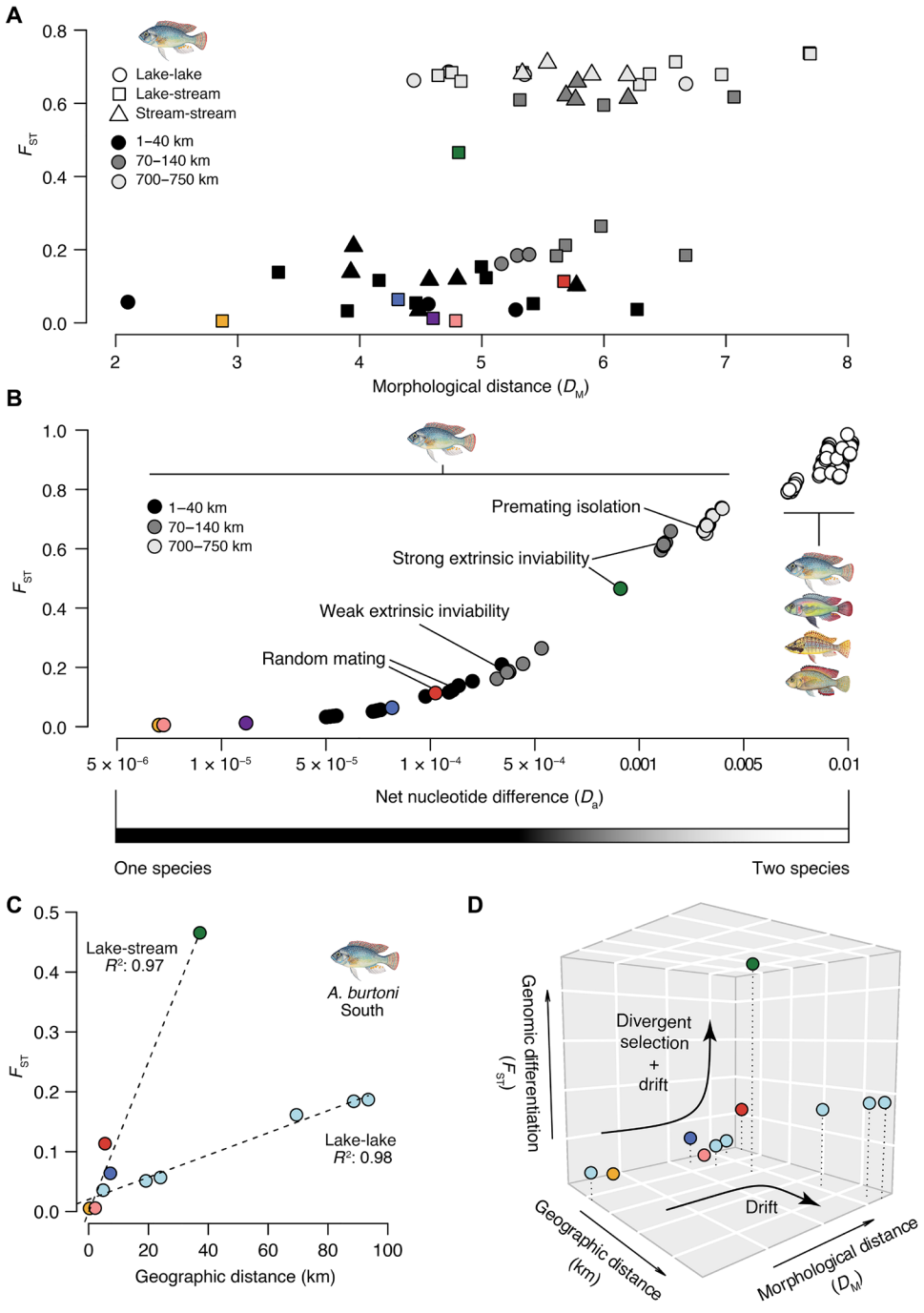

Fig. 2. Dynamics of diversification in *A. burtoni*. (**A**) Genome-wide F_{ST} between *A. burtoni* populations plotted against D_M calculated from body shape data. Geographic distance between populations and habitat type for each comparison are highlighted with symbol color and shape, respectively. The sympatric lake-stream systems are colored using the same color coding as in Fig. 1. Morphological distances increase gradually, whereas two groups of genetic distances are observed: the one-species ($F_{ST} < 0.3$) and the two-species ($F_{ST} > 0.6$) categories. (**B**) Genome-wide F_{ST} plotted against the net nucleotide difference [$D_a = d_{XY} - (\pi_1 + \pi_2)/2$; note the log-scale for the *x* axis to which the gray shading has been adjusted] in *A. burtoni* populations, covering the entire speciation continuum. Genomic differentiation accumulated rapidly during early stages of divergence ($F_{ST} < 0.3$; that is, the one-species category) but then slowed down as D_a increases ($F_{ST} > 0.6$; that is, the two-species category). Levels of reproductive isolation increase along a continuum of genomic differentiation (see Table 1 for details on the experiments and population used). (**C**) Isolation by distance in the two comparison categories lake-stream (the color coding for lake-stream systems is the same as in Fig. 1) and lake-lake (light blue) in the southern populations of *A. burtoni* (that is, within the one-species category). R^2, Pearson's correlation coefficient. (**D**) Trajectories for three differentiation axes: morphology, geography, and genetics. In lake-stream comparisons, morphological differentiation builds up first, and then genomic differentiation increases sharply. In contrast, in the absence of strong divergent selection (that is, in the lake-lake comparisons), morphological differentiation builds up first, and then genomic differentiation accumulates only moderately. All pairwise comparisons are represented with circles in (B) to (D).

Table 1. Summary of experimental testing for reproductive isolation in *A. burtoni*.

Populations	F_{ST}	Genetic markers	Experimental setup	Main results	Reproductive isolation	Reference
Kalambo lake × Kalambo River 2	0.113	Whole genome	Transplant experiment in the lake environment	Adaptive phenotypic plasticity	Weak for wild-caught adults; not observed for F1	(*27*)
Kalambo lake × Lunzua River	0.123	Whole genome	Common garden experiment in mesocosms	Random mating	Not observed	(*20*)
Kalambo lake × Ndole lake	0.189*	Whole genome*	Common garden experiment in mesocosms	Immigrant and extrinsic hybrid inviability (weak)	Extrinsic prezygotic and postzygotic isolation (weak)	(*28*)
Ndole lake × Lufubu River	0.472*	Whole genome*	Common garden experiment in mesocosms	Immigrant and extrinsic hybrid inviability (strong)	Extrinsic prezygotic and postzygotic isolation (strong)	(*28*)
Kalambo lake × Lufubu River	0.624	Whole genome	Common garden experiment in mesocosms	Immigrant and extrinsic hybrid inviability (strong)	Extrinsic prezygotic and postzygotic isolation (strong)	(*28*)
Kalambo lake × Rusizi lake	0.693	Whole genome	Laboratory mate-choice experiment	Partial assortative mating	Premating isolation	This study

*Genetic distances inferred from the Lufubu lake population rather than Ndole lake population [both populations are geographically close and belong to the same genetic cluster (*20*)].

isolation between population pairs were significant (*28*). Thus, there is evidence for reproductive isolation between populations in the gray zone of speciation and in the two-species category, indicating that our species categories that are solely based on levels of genome-wide differentiation in *A. burtoni* are biologically meaningful. In support of this, our new laboratory-based mate-choice experiments targeting two populations that feature one of the highest genome-wide F_{ST} values (Kalambo lake versus Rusizi lake: F_{ST} = 0.69) revealed signatures of assortative mating with respect to source population, at least in a multisensory laboratory setting, allowing for a combination of mating cues (see Supplementary Text and fig. S4).

Divergent selection and drift accelerate genome-wide differentiation

We then investigated the relative contribution of divergent selection and geography on genomic and morphological diversification in *A. burtoni*. To do so, we compared the more closely related South-West and East-West populations of *A. burtoni*, focusing on within habitat (lake-lake) versus between habitat (lake-stream) comparisons. The latter consisted of the five lake-stream systems (i.e., Chitili, Kalambo 1, Lunzua, Kalambo 2, and Lufubu) (Fig. 1B), whereas the lake-lake comparisons consisted of all pairwise comparisons of lake populations from that area. In both cases, we found an increase in F_{ST} over geographic distance (Fig. 2C), which is compatible with an isolation-by-distance scenario for lake-stream (linear regression, $P = 0.0013$; Pearson correlation coefficient, $R^2 = 0.97$) and lake-lake (Mantel test, P = 0.08; Pearson correlation coefficient, R^2 = 0.98) contrasts. Genomic differentiation increased much more strongly with respect to geographic distance when populations were compared that inhabit contrasting environments (lake-stream population comparisons, i.e., in the presence of divergent selection and drift) than when they inhabit similar environments (lake-lake comparisons, i.e., primarily in the presence of drift) (Fig. 2C). Such a signature has previously been shown in threespine sticklebacks (*29*).

We also performed demographic modeling of all lake-stream population pairs to test different scenarios of divergence and to infer demographic parameters such as population size and the extent of gene flow between lake and stream populations. We found that there is ongoing gene flow between lake and stream fish in all population pairs (fig. S3 and table S4) and that the effective population size of most stream populations was much smaller than that of the respective lake population (table S4), which is compatible with the scenario that the rivers were colonized from the respective lake stocks (*20*, *23*). As the impact of genetic drift is stronger in small populations, drift may also have contributed to the increased genomic divergence of stream populations. We found that morphological differentiation built up first at small genetic and geographic distances (Fig. 2D) and that genomic differentiation built up much more rapidly compared to geographic distance in the presence of divergent selection and increased drift (lake-stream comparisons) (Fig. 2D). This highlights that the environment (via divergent selection) and demographic events play a crucial role in differentiation trajectories in *A. burtoni*.

Little overlap between differentiation regions among independent lake-stream systems

We then turned our attention to the question of parallel morphological and genomic evolution along a lake-stream environmental contrast in cichlids. To do so, we compared all lake-stream population pairs from the four species to also include between-species comparisons. At the morphological level, we found that in eight of the nine lake-stream population pairs, lake fish had on average deeper bodies than river fish (Fig. 3A). A clustering analysis in *A. burtoni*

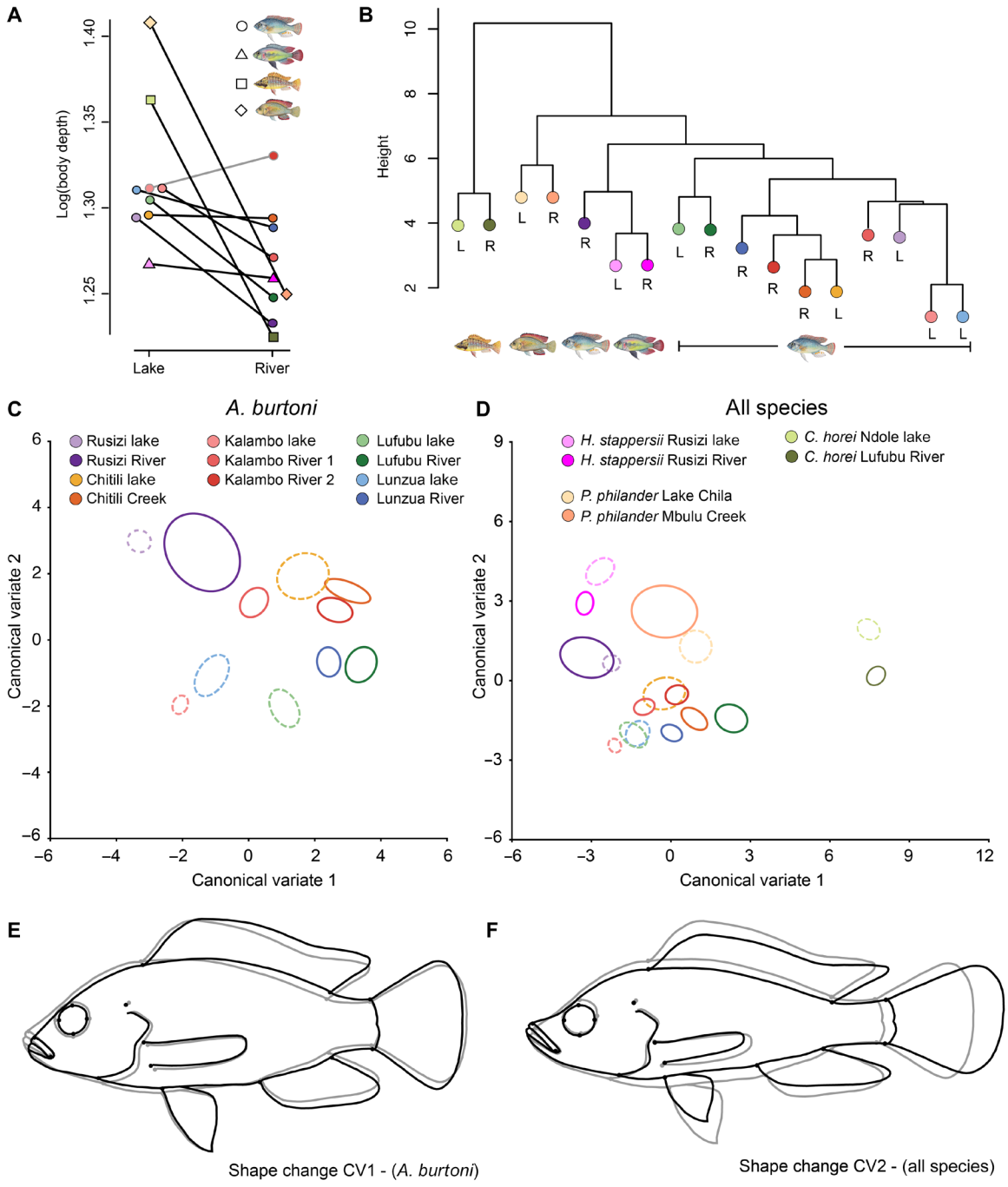

Fig. 3. Body shape variation among nine lake-stream population pairs from four cichlid species: *A. burtoni* (*N* = 289), *H. stappersii* (*N* = 81), *C. horei* (*N* = 67), and *P. philander* (*N* = 31). (**A**) Size-corrected comparison of average body depth among lake and river fishes. Black lines indicate decreasing value between lake and river populations. Gray line indicates increasing value between lake and river populations. (**B**) Dendrogram of body shape based on D_M among populations. Clustering algorithm, unweighted pair group method with arithmetic mean. (**C**) CVA of body shape for *A. burtoni*. Lake population outlines are shown in dashed lines, and river population outlines are shown in solid lines. (**D**) CVA of body shape for all species. Lake population outlines are shown in dashed lines, and river population outlines are shown in solid lines. (**E**) CV1 of shape change in *A. burtoni* only (scaling factor, 10; outlines are for illustration purposes only, from light gray to dark outlines with increasing values). (**F**) CV2 shape change for all four species (scaling factor, 10; outlines are for illustration purposes only, from light gray to dark outlines with increasing values).

revealed that, with the exceptions of Chitili lake and Kalambo River 1, populations clustered according to habitat and not to locality (Fig. 3B), suggesting the presence of two main ecotypes in this species, a "lake" and a "river" ecotype. This is further supported by a canonical variate analysis (CVA) (Fig. 3, C and E) and a principal components analysis (PCA; fig. S2), showing that *A. burtoni* lake-stream population pairs diverged along a common axis of morphological differentiation. Contrastingly, there was no such common

axis of morphological differentiation along the lake-stream contrast when all species were compared (Fig. 3, D and F).

At the genomic level, the *A. burtoni* lake-stream population pairs displayed contrasting levels of genome-wide differentiation, ranging from F_{ST} = 0.005 (Chitili) to F_{ST} = 0.465 (Lufubu) (Fig. 4). Differentiation between lake-stream population pairs in the other species ranged from low (*H. stappersii*; F_{ST} = 0.046) to intermediate (*C. horei*; F_{ST} = 0.532) to high (*P. philander*; F_{ST} = 0.733), corroborating that the two *P. philander* populations may actually represent two distinct species, as, for example, suggested by their different sex-determining systems (*26*). Consistent with this, the *P. philander* populations display relatively high levels of absolute divergence ($d_{XY} = 3.6 \times 10^{-3}$), which are above the levels of divergence measured between the northern and southern lineages in *A. burtoni* ($d_{XY} = 3.0 \times 10^{-3}$ to 3.3×10^{-3}) (Table 2).

We next investigated genomic regions of high differentiation between lake-stream population pairs and evaluated to which extent these outlier regions (defined here conservatively as the intersection between the top 5% 10-kb windows with respect to F_{ST}, d_{XY}, and absolute value of π difference) are shared between population pairs and species. Our analyses revealed between 2 and 101 outlier regions of high differentiation per lake-stream population pair and that these regions were between 10 to 70 kb in length (red dots in Fig. 4 and table S5). It has previously been shown that heterogeneity in crossover rates can produce contrasting patterns of genomic differentiation between diverging populations that are not due to divergent selection. These are manifested, for example, in greater levels of differentiation near chromosome centers (where crossover rates are lower) compared to the peripheries (where crossover rates are higher) (*30*). In our case, we did not find evidence for an accumulation of differentiation regions in the chromosome centers in any of the lake-stream population pairs, nor when all 525 outlier regions were considered jointly (table S5), suggesting that our results reflect true signatures of divergent selection.

We then evaluated to what extent differentiation regions were shared among lake-stream population pairs and species. We found that there was little overlap (Fig. 5A) and that no such region of high differentiation was shared between more than two population pairs (Fig. 5A). The regions of high differentiation were distributed across all linkage groups, although there seemed to be an overrepresentation on LG3 (64 of 525), which remained when correcting for chromosome length (table S5). The 525 differentiation regions contained a total of 637 genes. There was no obvious overrepresentation in functional enrichment with respect to Gene Ontology (GO) categories. The only exception was the Lunzua lake-stream comparison, in which outlier genes were significantly enriched for the molecular function "binding" (table S6). The 25 genes located in the 19 differentiation regions shared between two systems also showed no functional enrichment (table S7).

In situations of a shared evolutionary history of the populations under investigation, such as in our setup, frequency-based outlier detection methods may not represent the most appropriate strategy to detect regions under selection. Thus, we also performed Bayesian analyses of selection at the single-nucleotide polymorphism (SNP) level that take into account population relatedness (*31*). Because of their high levels of genome-wide differentiation, the population pairs of *C. horei* and *P. philander* were excluded from these analyses, as signatures of selection and drift cannot easily be disentangled in these cases. For the same reason, we treated the northern and southern populations of *A. burtoni* as separate units. We identified 1704 shared 10-kb windows of differentiation between *A. burtoni* from the South and *H. stappersii*, 1683 shared windows between *A. burtoni* from the North and *H. stappersii*, and 1542 shared windows between *A. burtoni* from the North and the South (Fig. 5B). In total, 373 windows were shared among the three core sets, containing 367 genes (Fig. 5B and table S8). Genes involved in sensory perception (sound and light) were overrepresented in the common set of outliers between *H. stappersii* and the southern *A. burtoni* populations.

The extent of parallel evolution in lake-stream divergence

We further aimed to quantify the extent of phenotypic and genomic parallel evolution among lake-stream pairs. To examine how (non-) parallel the nine lake-stream population pairs are, we performed vector analyses (*13*, *32*) using the morphological (37 traits and landmarks representing body shape) and genomic (outlier and non-outlier SNPs) data at hand (outlier SNPs: BayPass outliers, based on 78 principal components (PCs) from a genomic PCA, potentially affected by natural selection; non-outlier SNPs: all SNPs but excluding BayPass outliers). Following Stuart *et al.* (*33*), we quantified variation in lake-stream divergence by calculating vectors of phenotypic and genomic differentiation for each lake-stream population pair, whereby the length of a vector (L) represents the magnitude of lake-stream divergence and the angle between two vectors (θ) informs about the directionality of divergence. Accordingly, two lake-stream systems are more "parallel" if θ is small (similar direction of divergence) and ΔL (difference in length between two vectors) is close to zero (similar magnitude of divergence) (*13*).

Most comparisons between independent lake-stream population pairs fell into the category "nonparallel," with close to orthogonal (~90°) angles of differentiation in both phenotype (θ_P) and genotype ($\theta_{G\_outlier}$ and θ_G) (Fig. 5, F and I, and fig. S5D). However, parallelism was higher when only the within *A. burtoni* comparisons were considered, with values of θ_P and $\theta_{G\_outlier}$ between 70° and 80° in many cases (Fig. 5, F and I), but not for θ_G (fig. S5D). More clear signatures of parallelism were found in closely related *A. burtoni* lake-stream systems, with Lunzua–Kalambo 1 being the most parallel system at the phenotype level (θ_P, 42°) and Chitili–Kalambo 1 at the genotype level ($\theta_{G\_outlier}$, 26°). Overall, the directions of phenotypic (θ_P) and genetic ($\theta_{G\_outlier}$) differentiations were significantly positively correlated (Mantel test, P = 0.0075; Pearson correlation coefficient, R^2 = 0.27; Fig. 5C), whereas their magnitudes were not (Mantel test ΔL_P and $\Delta L_{G\_outlier}$, P = 0.26; linear regression model L_P and $L_{G\_outlier}$, P = 0.55; Fig. 5, D and E). In contrast, none of the non-outlier genetic vectors were correlated to phenotypic vectors (θ_P versus θ_G and ΔL_P versus ΔL_G: Mantel tests, P = 0.34; P = 0.35; L_P and L_G: linear regression, P = 0.93; fig. S5, A to C).

It has recently been proposed to examine the vectors of divergence using a multivariate approach as a complementary set of analyses to investigate (non-)parallelism and convergence (*34*). For each dataset (phenotype, genotype outlier, and genotype non-outlier), we thus calculated the eigen decomposition of the respective C matrix (m lake-stream systems × n traits). For the phenotypic data, we found that the first eigenvector (or PC) encompassed about 33% of the total phenotypic variance, which was significantly higher than expected under the null Wishart distribution (Fig. 5G). That is, there was one dimension of shared evolutionary change that

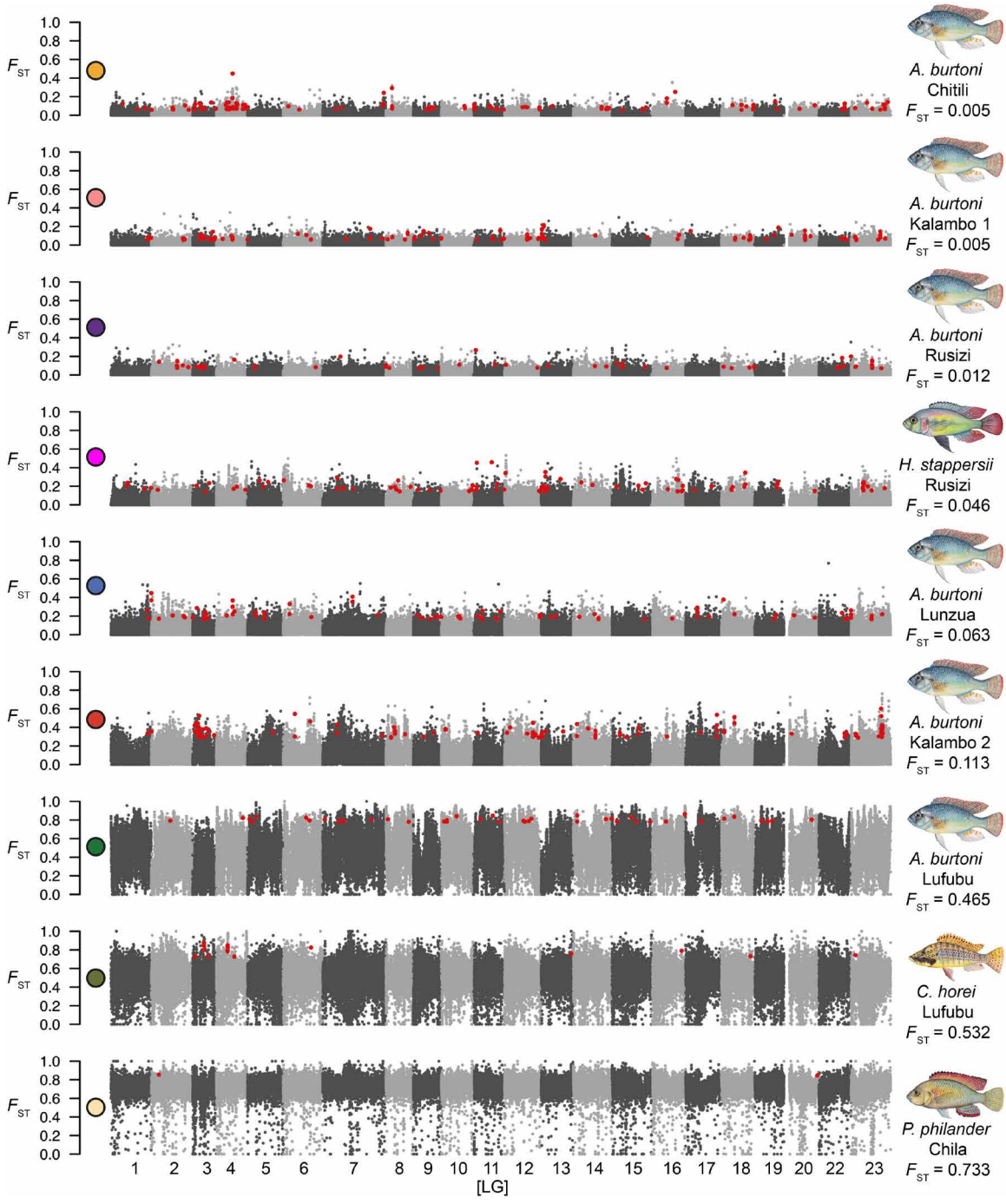

Fig. 4. Distribution of genome-wide F_{ST} for the nine lake-stream systems sorted by increasing genome-wide F_{ST} values. Each dot represents an F_{ST} value calculated in a 10-kb window along a given linkage group (L_G). Linkage groups are highlighted in different shades of gray. Regions of differentiation (overlap of the top 5% values of F_{ST}, d_{XY}, and π) are highlighted in red.

contained significant parallelism. We next examined whether the different lake-stream systems evolve in parallel or antiparallel directions by examining the loading of each PC, where a shared sign (positive or negative) is indicative of parallel evolution (*34*). The *H. stappersii* and the *P. philander* lake-stream systems had positive loadings, while all remaining seven lake-stream systems (all *A. burtoni* and *C. horei*) had a negative loading on their first PC axes. This indicates that all *A. burtoni* and *C. horei* systems evolve in parallel but in an antiparallel direction compared to *H. stappersii* and *P. philander*. Therefore, we detected both parallel and antiparallel evolution in the divergence of the four cichlid species along a similar environmental contrast. To infer which phenotypic characteristics were evolving in parallel among the different lake-stream systems, we examined which landmarks were contributing the most

Table 2. d_{XY} values between divergent populations and species used in this study. d_{XY} values are presented as a 10^{-3} factor for readability. The category *A. burtoni* "South" included all populations from southeast of Lake Tanganyika and the Lufubu lake population. *A. burtoni* "Lufubu" included the Lufubu River population. *A. burtoni* "North" included both populations (Rusizi lake and Rusizi River) from the North of Lake Tanganyika.

	***A. burtoni* South**	***A. burtoni* Lufubu**	***A. burtoni* North**	***H. stappersii***	***C. horei***	***P. philander***
A. burtoni South	0.9–1.3					
A. burtoni Lufubu	1.7–2.1	0				
A. burtoni North	3.0–3.2	3.3	1.0			
H. stappersii	6.7–6.8	6.7	6.4–6.5	1.6		
C. horei	8.4–8.5	8.4–8.5	8.4–8.5	8.5–8.7	1.1	
P. philander	10.5–10.9	10.5–10.8	10.6–10.9	10.7–11.0	9.6–10.0	3.6

to the first PC axis by examining the loading of PC1. We found that the seven landmarks with the most extreme loading values (<−0.4 or >0.4) were related to mouth position (landmark y1), eye size (landmarks x4 and y5), and slenderness of the body (body depth/standard length ratio and landmarks y7, y8, and y9) (fig. S5, J and M).

When examining the genetic outlier data, we found that PC1 encompassed about 30% of the total genetic variance, which was significantly higher than expected under the null Wishart distribution (Fig. 5J). The signs of the PC1 loadings (positive or negative) were the same in each lake-stream system as in the phenotypic data, namely, positive for *H. stappersii* and *P. philander* and negative for the remaining seven lake-stream systems. This again highlights parallel and antiparallel components in lake-stream divergence. Among the eight PCs of the genetic outliers with the most extreme loading values (<−0.3 or >0.3), four PCs (PC5, PC7, PC10, and PC11) were separating lake and stream populations (fig. S5, K and N). This indicates that half of the PCs contributing to genetic parallelism are involved in lake-stream divergence. Last, when examining the genetic non-outlier data, we found that the first PC encompassed about 25% of the total genetic (non-outlier) variance, which was also significantly higher than expected under the null Wishart distribution (fig. S5E). However, the interpretation of parallelism in the context of genetic non-outliers is less straightforward, as the seven genetic non-outlier PCs with the most extreme loading values (<−0.3 or >0.3) were not related to lake-stream divergence but rather to species separation or to divergence between the *H. stappersii* populations (fig. S5, L and O).

Parallelism is higher when ancestral populations are more similar

We then examined whether the degree of similarity in the ancestral lake populations correlates with the extent of morphological and genetic parallelisms. We found a significant positive correlation in both datasets, with a stronger effect in the genetic compared to the morphological data (Mantel tests: $\theta_{G\_outlier}$ versus F_{ST}, $P = 0.0039$; θ_P versus D_M, $P = 0.045$; $R^2 = 0.46$ and 0.17, respectively) (Fig. 5, H and K). This indicates that phenotypic and genetic parallelisms are higher when ancestral populations are phenotypically and genetically more similar. The genetic non-outliers (that is, the neutral markers) did not reveal such a correlation (Mantel test: θ_G versus F_{ST}, $P = 0.48$; fig. S5F). We also found that the proportion of standing genetic variation between ancestral populations was negatively correlated with θ_P and $\theta_{G\_outlier}$ (Mantel tests, $P = 0.0061$ and 0.0117; $R^2 = 0.32$ and 0.43, respectively) (fig. S5, G and H), but not with θ_G (Mantel test, $P = 0.19$; fig. S5I), indicating that lake-stream population pairs sharing larger amounts of standing genetic variation display more parallelism at the level of both phenotype and genotype.

Body shape convergence in species inhabiting the same rivers

We lastly assessed the levels of convergence (and divergence) in phenotype and genotype across all lake-stream systems. To do so, we first examined how genomic differentiation scales with morphological differentiation across species. We thus contrasted the levels of absolute genomic (d_{XY}) and morphological (D_M) differentiation between all *A. burtoni* populations and those of the three other species, resulting in 136 pairwise comparisons. We used d_{XY} rather than F_{ST} here, as d_{XY} is an absolute measure of genomic differentiation that is better suited for between-species comparisons. As above, we classified these comparisons according to the environmental contrasts (lake-lake, lake-stream, and stream-stream). The extent of body shape differentiation was only partially in agreement with the respective levels of genome-wide divergence (Fig. 6A). For example, the population pair from the Kalambo River involving the upstream population (*A. burtoni* Kalambo 2, $D_M = 5.6$) was morphologically more distinct than the between-species comparisons in the Rusizi River (*A. burtoni* versus *H. stappersii*, $D_M = 4.1$). In agreement with the levels of genomic differentiation ($d_{XY} = 3.6 \times 10^{-3}$), morphological differentiation was high in the *P. philander* population pair ($D_M = 6.0$).

We then calculated the among-lineage covariance matrices of mean trait values $\mathbf{D}_{river}$ and $\mathbf{D}_{lake}$ for each dataset (phenotype, genotype outlier, and genotype non-outlier) to investigate the levels of convergence and divergence in lake-stream differentiation. Following the definition of De Lisle and Bolnick (*34*), less variance in $\mathbf{D}_{river}$ compared to $\mathbf{D}_{lake}$ is indicative of convergent evolution, while more variance in $\mathbf{D}_{river}$ compared to $\mathbf{D}_{lake}$ is indicative of divergent evolution. We found divergence at the genomic level in both "outlier" and "non-outlier" datasets since trace subtraction $[\mathrm{tr}(\mathbf{D}_{river}) - \mathrm{tr}(\mathbf{D}_{lake})]$ was positive in both cases. In contrast, we found convergence at the phenotypic level since the result of trace subtraction was negative. In this latter case, two traits encompassed more than 99% of the total variance, namely, centroid size (66%) and total length (33%). This might be explained by the fact that the different traits and landmarks have different units accounting differently for the total amount of variance (e.g., variation in total length is measured in millimeters that ranges from 42 to 73, while

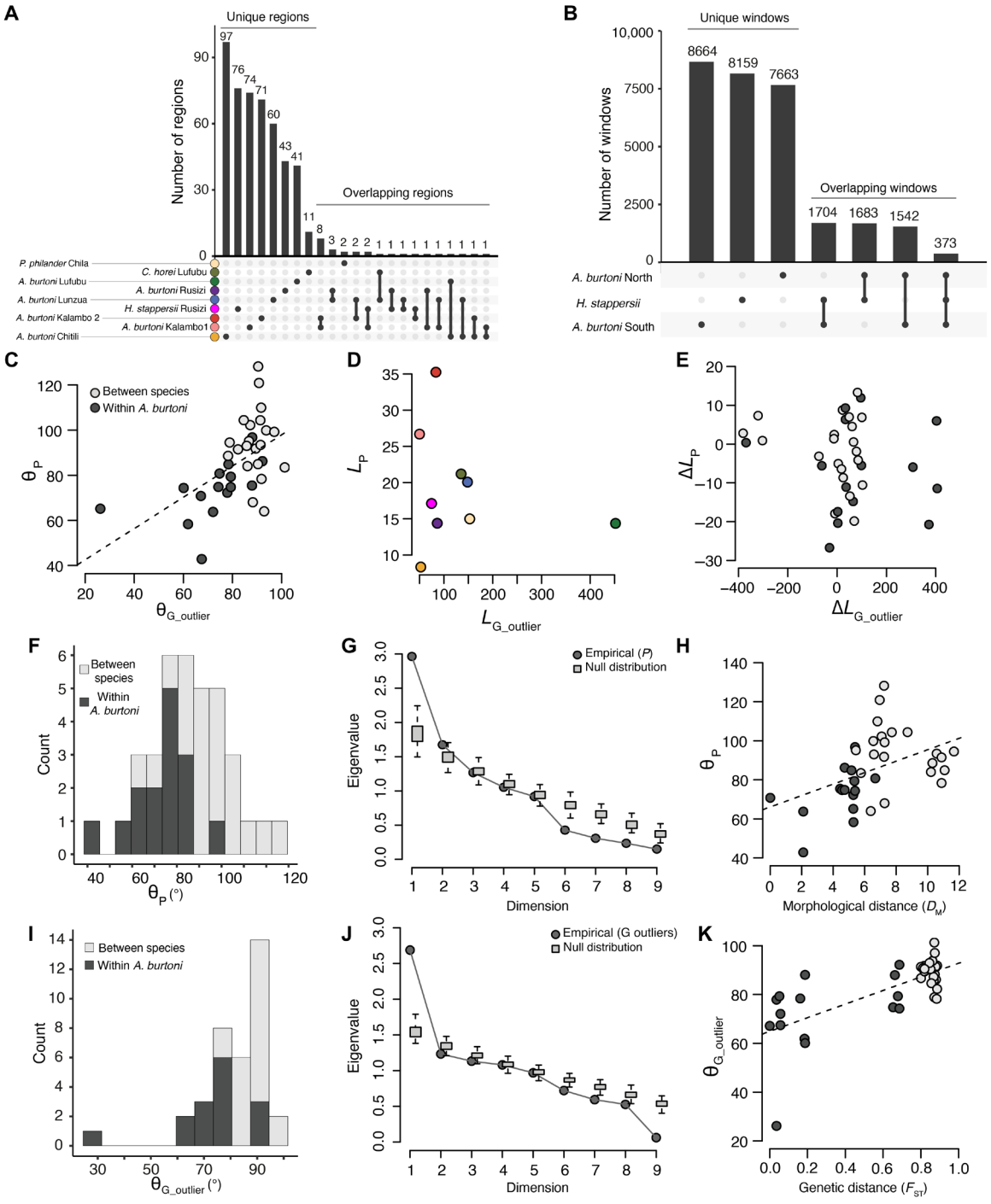

Fig. 5. Extent of parallel evolution among nine lake-stream cichlid population pairs. (**A**) Number of unique and overlapping differentiation regions (overlap of top 5% values of F_{ST}, d_{XY}, and π) in the nine lake-stream population pairs. (**B**) Number of unique and overlapping differentiation windows in the three sets of genomic outliers from BayPass in *A. burtoni* from the North of Lake Tanganyika, *A. burtoni* from the South, and *H. stappersii*. (**C**) The angles of phenotypic (θ_P) and genetic outlier ($\theta_{G\_outlier}$) lake-stream divergence vectors are positively correlated (Mantel test, $P = 0.0075$; Pearson correlation coefficient, $R^2 = 0.27$). (**D**) The lengths of phenotypic (L_P) and genetic outlier ($L_{G\_outlier}$) lake-stream divergence vectors were not correlated (linear regression model, $P = 0.55$). The color scheme is the same as in (A). (**E**) The differences between phenotypic (ΔL_P) and genetic outlier ($\Delta L_{G\_outlier}$) vector length were not correlated (Mantel test, $P = 0.26$). (**F**) Histogram of pairwise angles between lake-stream phenotypic divergence vectors (θ_P) in degrees. (**G**) A multivariate analysis of phenotypic parallelism revealed one significant dimension of parallel evolution. (**H**) The angles of phenotypic divergence vectors (θ_P) and morphological distances (D_M) between ancestral (i.e., lake) populations were positively correlated (Mantel test, $P = 0.045$; $R^2 = 0.17$). (**I**) Histogram of pairwise angles between lake-stream genetic outlier divergence vectors ($\theta_{G\_outlier}$) in degrees. (**J**) A multivariate analysis of genetic parallelism revealed one significant dimension of parallel evolution. (**K**) The angles of genetic outlier divergence vectors ($\theta_{G\_outlier}$) and genetic (F_{ST}) distances between lake populations were positively correlated (Mantel test, $P = 0.0039$; $R^2 = 0.46$).

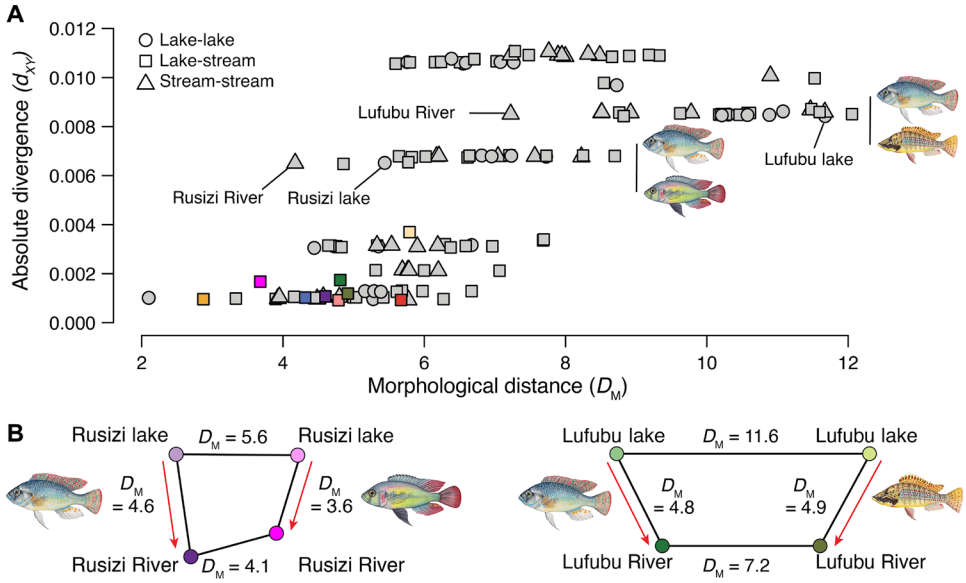

Fig. 6. Body shape convergence among sympatric species pairs. (**A**) Absolute divergence (d_{XY}) plotted against morphological distance (D_M) for 136 pairwise comparisons across all populations from the four species used in this study. A wide range of morphological distances can be observed for the same amount of genomic divergence. The sympatric populations (*A. burtoni* and *H. stappersii* from the Rusizi system; *A. burtoni* and *C. horei* from the Lufubu system) are highlighted. The habitat type for each comparison is indicated with different symbols (circle, square, and triangle). The color scheme is the same as in Fig. 5A. (**B**) Smaller morphological distances between sympatric riverine populations compared to sympatric lake populations revealed body shape convergence in the riverine populations (*A. burtoni* and *H. stappersii* from the Rusizi system; *A. burtoni* and *C. horei* from the Lufubu system).

variation in landmarks is measured in Procrustes units that ranges from −0.3 to 0.4). This inherent issue to the method has been identified by De Lisle and Bolnick (*34*) and references therein.

A more intuitive and biologically more meaningful way to assess convergence versus divergence is to compare Euclidean distances for a specific trait. Thus, for each pair of lake-stream systems, we compared the D_M between the respective lake and the stream populations, where convergence is suggested when $D_{M\,river} - D_{M\,lake} < 0$, with a more negative value indicative of higher convergence (*34*). Within *A. burtoni*, the majority of pairwise comparisons indicated divergent evolution in body shape except for Chitili/Kalambo 1 and Chitili/Kalambo 2, with the highest level of convergence observed for the latter comparison (table S9). The between-species comparisons revealed mostly divergent evolution, except for comparisons between the southern populations of *A. burtoni* and *C. horei*, for which a signature of convergence was detected. The highest level of convergence was found between *A. burtoni* and *C. horei* sampled in sympatry in the Lufubu River. The lake populations were highly differentiated ($D_{M\,lake}$ = 11.6), representing one of the most divergent comparisons in terms of morphology across all comparisons (Fig. 6A). In contrast, *A. burtoni* and *C. horei* from Lufubu River were morphologically rather similar ($D_{M\,river}$ = 7.2) given their high level of genome-wide divergence ($d_{XY} = 8.5 \times 10^{-3}$) (Fig. 6A) and similar levels of within-species lake-stream divergence (*A. burtoni*, D_M = 4.8; *C. horei*, D_M = 4.9) (Fig. 6B). Body shape convergence was also observed in the *A. burtoni* and *H. stappersii* populations from the Rusizi system. While the Rusizi lake populations were morphologically differentiated ($D_{M\,lake}$ = 5.4), the respective populations from Rusizi River were much more similar ($D_{M\,river}$ = 4.1) despite almost identical levels of genome-wide differentiation ($d_{XY} = 6.5 \times 10^{-3}$ for both comparisons) (Fig. 6B and Table 2). Moreover, the level of between-species morphological differentiation in the same river (D_M = 4.1) was smaller than the within *A. burtoni* differentiation in contrasting environments (D_M = 4.6) (Fig. 6B and table S3). Convergent evolution becomes even more evident in the clustering analysis, in which *A. burtoni* specimens from the Rusizi River clustered with *H. stappersii*, rather than with other *A. burtoni* populations (Fig. 3B). Thus, we observed body shape convergence in species that co-occur in the same river systems and, hence, diversified along the very same environmental contrast. We note that gene flow between species can be ruled out as the reason for the similarities between co-occurring species (figs. S6 and S7).

DISCUSSION

Morphological and genomic diversification in *A. burtoni*

The first aim of this study was to investigate the dynamics of morphological and genomic diversification in the cichlid species *A. burtoni*. Making use of body shape information of 289 specimens and whole-genome data of 132 individuals from six lake-stream population pairs displaying various levels of genome-wide divergence, we investigated how morphological and genomic differences accumulated along a lake-stream environmental contrast and across geographic distances. Consistent with previous findings based on restriction-site associated DNA sequencing (RAD-seq) data (*23*), we found that stream populations feature smaller effective population sizes than the respective lake populations (fig. S3), possibly reflecting founder effects and/or physical limitations in the riverine environment. When considering only the populations from the South of Lake Tanganyika, for which we had a denser geographic sampling (Fig. 1), it turned out that, at a given geographic distance, genomic differentiation is greater in lake-stream than in lake-lake population comparisons (Fig. 2C).

This suggests that in *A. burtoni*, genomic differentiation builds up more rapidly between populations in the presence of divergent selection and drift (i.e., in a lake-stream setting) compared to a situation dominated by only drift (i.e., in a lake-lake setting), at least over short geographic distances. Thus, it appears that the combined effect of divergent selection and genetic drift accelerate genome-wide differentiation in *A. burtoni*, just as has been reported for parapatric lake-stream population pairs of threespine sticklebacks (*29*). The pairwise population comparisons revealed that, in both settings (lake-lake and lake-stream), morphological differentiation increased rapidly over short geographic distances and at low levels of genetic distances (Fig. 2D). The substantial differences in body shape observed between closely related and geographically adjacent populations are likely to reflect adaptive variation on the basis of genetic and environmental factors (*20*, *35*).

Through the examination of the southern populations of *A. burtoni*, we could therefore establish that divergent natural selection together with genetic drift facilitates differentiation, but whether these forces are sufficient to complete speciation remains open. To address this question, we investigated the patterns of morphological and genomic differentiation across all available *A. burtoni* population pairs, which span a continuum of divergence ranging from virtually panmictic to population pairs that resemble separate species (Fig. 2). We found opposite results for morphological and genomic differentiation: While morphological differentiation was continuous (Fig. 2A), the population pairwise F_{ST} values fell into two main categories, the "one-species" category ($F_{ST} < 0.3$) and the "two-species" category ($F_{ST} > 0.6$), with a single population pair in between (Fig. 2B). The observed gap in genomic differentiation can only partially be explained by geographic distance. While pairwise F_{ST} values were smaller than 0.2 for geographic distances between the respective populations ranging from 1 to 40 km, F_{ST} values for geographic distances from 70 to 140 km were assigned into both categories. Overall, our results in cichlids are, thus, similar to what has been observed in *Timema* stick insects, in which comparable levels of genomic differentiation were found along an ecologically driven speciation continuum ($F_{ST} < 0.3$ in within-species population comparisons versus $F_{ST} > 0.7$ in between-species comparisons) (*6*). This suggests that there might be a certain threshold of genomic differentiation delimiting species. We note, however, that additional population pairs from additional taxa with different levels of genomic divergence should be investigated to confirm this pattern.

Reproductive isolation increases with genomic divergence

The second aim of our study was to assess to what extent genomic divergence scales with reproductive isolation. We therefore reviewed previous data that used the very same *A. burtoni* populations as in the present study and performed mate-choice experiments between the genetically most distinct *A. burtoni* populations from the North and the South of Lake Tanganyika. Assortative mating has not been detected between populations showing low levels of genomic differentiation (*20*, *27*). However, there is evidence for reproductive isolation via extrinsic inviability between parapatric and allopatric lake and stream populations with intermediate ($F_{ST} = 0.47$) and high ($F_{ST} = 0.62$) levels of genomic differentiation (Fig. 2B) (*28*). Furthermore, our new mate-choice experiments revealed that genetically highly distinct allopatric *A. burtoni* populations ($F_{ST} = 0.69$) show signatures of assortative mating in a setting including all cues [i.e., visual, olfactory and, possibly, acoustic; note that it has previously been shown that olfactory cues are more important than visual cues in *A. burtoni* mate choice (*36*)]. This suggests that premating reproductive isolation mechanisms are at play between the genetically most distinct *A. burtoni* clades, the northern and southern lineages (*24*), at a level of genomic differentiation that is similar to the one typically observed between other cichlid species (Fig. 2B). Together, the results from previous studies and our new experiment indicate that the extent of reproductive isolation between *A. burtoni* populations scales positively with their levels of genome-wide divergence, as has been shown for other taxa as well (*37*, *38*).

Rapid diversification in cichlid fishes

Compared to other organisms, reproductive isolation is in place between *A. burtoni* populations featuring low levels of net nucleotide divergence (D_a), which serves as a proxy of time since population divergence. For example, on the basis of the comparative analysis of 63 population or species pairs along a continuum of genomic divergence, Roux and coworkers (*39*) suggested the gray zone of speciation to correspond to D_a values ranging from 0.5 to 2%. In the case of *A. burtoni*, however, extrinsic inviability was detected for population pairs at D_a values ranging from 0.1 to 0.2% (*28*), and evidence for premating isolation was found at $D_a = 0.4\%$ (this study). While our results are not exactly comparable to (*39*) because of different ways of measuring reproductive isolation [gene flow modeling in (*39*) versus experiments in our study] and because D_a is a relative measure of genome differentiation depending on within-species genetic diversity, it nevertheless appears that reproductive barriers build up more rapidly in cichlids compared to other animals.

In line with this, in addition, the d_{XY} values as absolute measure of divergence were lower between cichlid species compared to other organisms. For example, the levels of absolute divergence between *A. burtoni* populations from the North and the South of Lake Tanganyika ($d_{XY} = 3.0 \times 10^{-3}$ to 3.2×10^{-3}) or between *A. burtoni* from the North and *H. stappersii* ($d_{XY} = 6.4 \times 10^{-3}$ to 6.5×10^{-3}) are smaller or similar than what has been reported between allopatric populations in one species of stickleback fish (*Pungitius sinensis*, $d_{XY} = 6.2 \times 10^{-3}$ to 9.8×10^{-3}) (*8*). One the other hand, the between-species d_{XY} values reported in this study are similar to those measured for 73 species representative of the adaptive radiation of cichlid fishes in Lake Malawi ($d_{XY} = 1.0 \times 10^{-3}$ to 2.4×10^{-3}) (*40*) and to those between two *Pundamilia* cichlid species pairs from Lake Victoria ("Python," $d_{XY} = 2.05 \times 10^{-3}$; "Makobe," $d_{XY} = 2.17 \times 10^{-3}$) (*41*). Together, this once again underpins the explosive nature of speciation in African cichlid fishes (*16*).

Is there a role for allopatry in the completion of speciation?

Considering the allopatric distribution of the three most divergent lineages of *A. burtoni* in Lake Tanganyika (southern, northern, and Lufubu River) (fig. S1), it appears possible that geographic separation could have facilitated their diversification. A phylogeographic analysis based on genome-wide markers has even suggested that the northern lineage of *A. burtoni* originated from a colonization event of the lake from the Lukuga River (a temporary outlet in the central western part of Lake Tanganyika), whereas the ancestors of the southern lineage may have colonized the lake through the Lufubu basin (*24*). Thus, it is possible that the initial divergence between the northern and the southern lineage of *A. burtoni* occurred outside Lake Tanganyika. We would like to note, however, that the evolutionary history of *A. burtoni* is complex with strong indications for past

hybridization events [for example, there are shared mitochondrial haplotypes between populations from the North and the South (*24*)], making it difficult to determine the relative contribution of allopatry in the diversification of populations. Nevertheless, in agreement with a role of allopatry, our demographic modeling for the divergent Lufubu lake-stream population pair in the "gray zone of speciation" suggested that, while there is ongoing gene flow, there likely was at least one period of allopatry in the past. Such a demographic scenario of secondary contact after isolation would be compatible with a complete separation between lake and stream populations during periods of low lake levels in Lake Tanganyika, during which the lake's shoreline was substantially shifted (*42*). While this would be in line with the view that allopatry contributes to the completion of speciation (*2*), we cannot, with the data at hand, conclusively answer the question about a possible role of allopatry in the divergence of *A. burtoni*.

Little overlap between regions of differentiation among lake-stream systems

The third aim of this study was to examine and quantify the levels of parallelism among the different lake-stream populations. The inspection of genomic regions of differentiation, defined here as overlap between the top 5% in F_{ST}, d_{XY}, and π, revealed that, with between 2 and 101 such regions, the number of outlier regions reported here is relatively small compared to other studies in cichlids (*41*, *43*). This can, however, be explained by our more stringent definition of such regions of differentiation (the intersection between three metrics). Overall, we found little overlap among the differentiation regions from different lake-stream systems. Only up to 19 outlier regions were shared between two lake-stream systems, and not a single such region was shared by more than two systems. However, the Bayesian analyses of selection revealed that *H. stappersii* and the southern *A. burtoni* populations shared a common set of overrepresented outlier loci involved in sensory perception (sound and light). This suggests that, although a large majority of the genomic outlier regions are not shared among systems, some functions appear to be particularly important for riverine adaptation and may, hence, repeatedly be the target of natural selection. Consistent with this, a previous study identified common highly differentiated genomic regions between a young and an old cichlid species pair diverging along a depth gradient in Lake Victoria, with two-thirds of the differentiation regions being private to each species pair (*41*). These results highlight that adaptive divergence often encompasses both parallel and system-specific (nonparallel) components.

The overall low levels of gene and function sharing among the different lake-stream systems reported here may partly be explained by cryptic environmental heterogeneity, as the rivers from which the populations were sampled differ in size and other environmental features, possibly requiring specific mechanisms of adaptation [e.g., (*33*)]. This may particularly be the case for the *P. philander* population pair, which was not sampled in Lake Tanganyika but in the small Lake Chila. A nonmutually exclusive explanation for the lack of sharing of regions of differentiation is that these regions may not be due to divergent selection but due to drift and background selection (*44*), as the majority of population pairs did not diversify under a demographic scenario of primary divergence with gene flow (fig. S3). This effect could have further been enhanced by the small effective population sizes of the riverine populations. On the other hand, background selection is realistic mainly for population pairs with elevated levels of genome-wide differentiation (*45*), which is not the case for some of the population pairs examined here. It is also possible that adaptive phenotypic plasticity (*27*, *46*) and epigenetic factors (*47*, *48*) play complementary roles during adaptive divergence. However, their investigation was beyond the scope of the present study.

Levels of parallelism in lake-stream divergence

To quantify the level of parallelism among the nine lake-stream systems, we performed phenotypic change vector analyses (*13*, *32*). Similar to what has previously been reported in lake-stream population pairs of threespine sticklebacks (*33*), we found that diversification was not particularly parallel among the different lake-stream systems, as the majority of θ_P and $\theta_{G\_outlier}$ values were close to orthogonal (Fig. 5, F and I). $\theta_{G\_outlier}$ values correlated with θ_P values, but $\theta_{G\_non\text{-}outlier}$ values did not. This strongly suggests that adaptive phenotypic divergence has a genetic basis in the species under investigation. Furthermore, we conducted a recently proposed multivariate analysis of the C matrix, which is essentially a PCA of (phenotypic or genomic) vectors of differentiation (*34*). We found that for both phenotypic and genomic outlier datasets, there was one significant axis of parallel evolutionary change, in which seven of nine lake-stream systems evolved in parallel. These seven lake-stream systems were the same in the phenotypic and in the genomic outlier datasets. That is, all *A. burtoni* and *C. horei* lake-stream systems have a common major axis of phenotypic and genomic parallel evolution, while *H. stappersii* and *P. philander* evolved in an antiparallel manner with regard to the seven other lake-stream systems (Fig. 5, G and J).

The traits underlying parallel phenotypic evolution were related to mouth position, eye size, and slenderness of the fish body, all of which have previously been suggested to contribute to adaptive divergence in *A. burtoni* (*20*). We show here that these phenotypic traits evolved in parallel not only in all *A. burtoni* lake-stream systems but also in *C. horei*. Furthermore, eight PCs contributing most to parallel genotypic evolution were related to lake-stream divergence (four PCs), species differences (three PCs), and geographic divergence within *A. burtoni* (one PC). Therefore, the genomic outliers mostly encompass candidate genomic loci for lake-stream adaptive divergence. Unexpectedly, the analysis of the genomic non-outliers also revealed a significant axis of parallel evolution. However, these genomic traits were not related to lake-stream divergence but rather summarized between-species (one PC), geographic (three PCs), or within-population (three PCs) divergence. This major axis of divergence may, hence, be the signature of drift under non-isotropic genetic variance (*34*).

The distance between ancestral populations determines the level of parallelism

It has previously been suggested that the probability of parallelism at the molecular level decreases with time since divergence (*49*). Furthermore, it has been suggested that the extent of parallelism should be higher when ancestral populations were closely related (*11*). We thus examined whether there was a correlation between the distances between ancestral (i.e., lake) populations and the level of parallelism in lake-stream divergence. We found that for both phenotypic and genetic outliers, there was a significant positive correlation between these metrics (θ_P and D_M; $\theta_{G\_outlier}$ and F_{ST}; Fig. 5, H and K), corroborating the view that the morphological and

genetic distances between ancestral populations influence the level of parallelism.

Standing genetic variation is an essential component in replicated adaptive evolution (*50*). Thus, we also tested whether the amount of standing genetic variation between ancestral populations was correlated to the levels of parallelism in the respective lake-stream systems. In line with our predictions, we found that the levels of standing genetic variation and parallelism were negatively correlated (fig. S5, G and H). That is, lake-stream population pairs sharing larger amounts of standing genetic variation display more parallelism at the level of both the phenotype and the genotype. Parallelism is, thus, likely constrained by the amount of standing genetic variation upon which natural selection can act, as the effect of de novo beneficial mutations on parallel evolution is much less likely to play an important role in the rapid adaptive divergence of recently evolved population pairs. Previous theoretical work has further shown that even small differences in the directionality of selection can greatly reduce genetic parallelism, especially in the case of complex traits (*51*). This suggests that, besides time since divergence, cryptic habitat heterogeneity also (leading to small differences in the directionality of selection) can decrease the likelihood of parallelism. In support of this, a comparison of regional (within Vancouver Island) versus global (North America versus Europe) lake-stream population pairs of sticklebacks showed that parallelism was lower at increased spatial scales, with global replicates showing less parallelism (*52*).

Body shape convergence between sympatric species pairs

Last, we investigated levels of convergence or divergence among the nine lake-stream population pairs. While we found divergence at the genomic levels (for both outlier and non-outlier datasets), we found convergence at the morphological level (Fig. 6B). We found body shape convergence in both species pairs coinhabiting the same river systems, namely, *A. burtoni* and *H. stappersii* in the Rusizi River and *A. burtoni* and *C. horei* in the Lufubu River (Fig. 6B) (also note that the sympatric population pairs show rather similar F_{ST} values across species; Fig. 3). This highlights that local selection regimes constrain body shape evolution in cichlids. This has previously been shown in Midas cichlids (*Amphilophus* sp.), where the body shapes of two syntopic species were more similar to one other than the body shape average of the first species from different localities (*53*).

That we did not find convergence at the genomic level may be due to several nonmutually exclusive factors. For example, the outlier detection method based on lake-stream differences might not be the most appropriate to uncover the genomic basis of morphological evolution. A quantitative traits loci approach might be more suitable here, as has previously been applied to uncover genomic regions underlying body shape differences along a benthic-limnetic axis of Midas cichlids (*54*, *55*). Further, adaptive phenotypic plasticity may also play a role in body shape evolution, as has recently been suggested for *A. burtoni* (*20*, *27*, *46*). Future studies should thus focus on quantifying the respective influence of genomic divergence versus phenotypic plasticity in adaptive divergence.

CONCLUSION

By examining the dynamics of differentiation in the African cichlid *A. burtoni*, we found that morphological differentiation was continuous along the speciation continuum. Contrastingly, we detected a gap in genomic differentiation that was only partially explained by geographic patterns. Our results, therefore, provide additional support for the hypothesis that there is a tipping point in genomic differentiation during the speciation process (*5*), suggesting that there might be a threshold of genomic differentiation to delimit species. We further showed that genomic differentiation was accelerated in the presence of both divergent selection and genetic drift, highlighting the combined effect of selective and neutral processes in speciation.

To gain insights into the potential predictability of the speciation process, we investigated the extent of parallel evolution in nine population pairs from four cichlid species that diverged along a similar lake-stream environmental contrast. While pairwise comparisons failed to identify strong signatures of phenotypic and genomic parallelism, multivariate analyses uncovered major axes of shared evolutionary changes along the lake-stream contrast. Last, we found that levels of parallelism were higher between closely related and, hence, genetically more similar population pairs. While the speciation process is overall difficult to predict, our results support the view that evolution can be predictable to a certain extent if appropriate models and data are used (*56*). To conclude, our study corroborates that contingency plays an important role in speciation and that speciation is a complex product of differentiation trajectories through multivariate space and time.

MATERIALS AND METHODS

Study design

Research objectives

In this study, we investigated the dynamics of morphological and genomic diversification in *A. burtoni* populations that have diverged along a lake-stream environmental contrast and across geography. We further aimed to investigate the extent and predictability of (non-) parallelism and convergence in nine lake-stream population pairs from four East African cichlid species.

Research subjects or units of investigation

There were four cichlid species: *A. burtoni*, *C. horei*, *H. stappersii*, and *P. philander*.

Experimental design

Individuals of *A. burtoni* ($N = 132$), *C. horei* ($N = 24$), *H. stappersii* ($N = 24$), and *P. philander* ($N = 24$) were collected in Zambia and Burundi between January and November 2015 (tables S1 and S2). All fishes were sampled with a ~1:1 sex ratio and were adult specimens except for three *P. philander* juveniles from the Mbulu River. Fishes were sampled in six different tributaries to Lake Tanganyika, whereby each system comprises a riverine population ($N = 10$ to 12) and a lake population ($N = 12$ to 14) and was named after the river, except for the Lake Chila system that was sampled outside the Lake Tanganyika basin. *H. stappersii* were sampled at the Rusizi River, in the North of Lake Tanganyika, along with sympatric *A. burtoni* (Fig. 1 and table S1). All other populations were sampled in the South of Lake Tanganyika. *A. burtoni* and *C. horei* were sampled at the Lufubu River; *A. burtoni* was further sampled in the Lunzua, Chitili, and Kalambo rivers (Fig. 1 and table S1). As two river populations were sampled in the Kalambo River, two lake-stream population comparisons were used for this river, namely, Kalambo 1 (comparison Kalambo lake versus Kalambo 1) and Kalambo 2 (comparison Kalambo lake versus Kalambo 2). Last, *P. philander* were sampled in small Lake Chila and in Mbulu creek (Fig. 1 and table S1). All fishes were caught with fishing rods or minnow traps

and anesthetized using clove oil. Photographs of the left lateral side were taken using a Nikon D5000 digital camera, under standardized lighting conditions, and with a ruler as a scale. To aid in digital landmark placement, three metal clips were used to spread the fins at the anterior insertions of the dorsal and anal fin and at the insertion of the pectoral fin (fig. S2A). To increase the sample size for morphological analyses, additional individuals were sampled and photographed at the same locations and time points as the individuals whose genomes were sequenced (table S2). Standard length, total length, and weight were measured. A piece of fin clip was preserved in 99% ethanol for DNA extraction. Whole specimens were preserved in 70% ethanol.

Sample size

For the genomic analyses, we intended to sample 12 individuals per population (6 males and 6 females), as 24 alleles per population are sufficient to obtain accurate allele frequency estimates. We sampled only 10 *A. burtoni* specimens from the Rusizi River because we did not succeed in catching additional specimens after numerous attempts. To compensate, 14 *A. burtoni* specimens from Rusizi lake were sampled to obtain a total of 24 *A. burtoni* specimens from the Rusizi lake-stream system. For the morphometric analyses, we intended to photograph at least 17 specimens per population, which is equal to the number of landmarks used. Fewer specimens were photographed in three populations (*A. burtoni* Chitili lake, $N = 13$; *A. burtoni* Rusizi River, $N = 10$; *P. philander* Mbulu Creek, $N = 9$) because we did not succeed in catching additional specimens after numerous attempts and because three of the individuals caught in Mbulu Creek were juveniles and, thus, excluded from the morphometric analyses.

Data inclusion/exclusion criteria and outliers

For the genomic analyses, all individuals were included in the analyses except one hybrid specimen between *A. burtoni* and another species that was detected only after whole-genome sequencing. For the morphometric analyses, juveniles were excluded on the basis that their morphology is different from the adults' morphology.

Replicates

The first mate-choice experiment (including only visual cues) was replicated 44 times; each replicate included one trio of fish (one female and two males from different populations). The second mate-choice experiment (including direct contact) was replicated eight times; each replicate included eight fish (two males and six females). Additional replicates could not be performed because of the limited number of fish available in the laboratory.

DNA extraction, sequencing, and data processing

DNA was extracted from fin clips using the E.Z.N.A. Tissue DNA Kit (Omega Bio-Tek) following the manufacturer's instructions. Individual genomic libraries were prepared using TruSeq DNA PCR-Free Low Sample Kit (Illumina) and subsequently sequenced [150–base pair (bp) paired-end] on an Illumina HiSeq 3000 sequencer at the Genomics Facility Basel operated jointly by the ETH-Zürich Department of Biosystems Science and Engineering and the University of Basel.

For each library, the quality of raw reads was visually inspected using FastQC (v0.11.3), and Illumina adapters were trimmed using Trimmomatic (v0.36). Filtered reads of each individual were aligned separately against the *Metriaclima zebra* reference genome (assembly M_zebra_UMD1). We chose this reference genome rather than the *A. burtoni* reference genome (*19*) to avoid any reference bias when comparing *A. burtoni* with the other species. We also chose *M. zebra* rather than *Oreochromis niloticus* as reference genome to maximize the number of reads mapped, as *M. zebra* is phylogenetically closer to *A. burtoni*, *C. horei*, *H. stappersii*, and *P. philander* than *O. niloticus*.

The *M. zebra* reference genome was indexed using Burrows-Wheeler Aligner (BWA; v.0.7.12), and alignments were performed using BWA-mem with default parameters. Obtained alignments in SAM format were coordinate-sorted and indexed using SAMtools (v.1.3.1). The average coverage per individual ranged from 9.8× to 24.5× (table S1). We performed an indel realignment using RealignerTargetCreator and IndelRealigner of the Genome Analysis Tool Kit (GATK; v3.4.0). Variants were called using the GATK functions HaplotypeCaller (per individual and per scaffold), GenotypeGVCFs (per scaffold), and CatVariants (to merge all VCF files). The VCF file corresponding to the mitochondrial genome (scaffold CM003499.1) was then isolated from the VCF file corresponding to the nuclear genome (that is, all other scaffolds). The latter was annotated with the features ExcessHet (that is, the Phred-scaled P value for an exact test of excess heterozygosity) and FisherStrand (that is, the strand bias estimated using Fisher's exact test) using the GATK function VariantAnnotator. To filter the VCF file, empirical distributions of depth (DP) and quality (QUAL) were examined. The VCF file was filtered using the GATK function VariantFiltration with the following values (variants meeting the criteria were excluded): DP < 2000, DP > 4000, QUAL<600, FisherStrand > 20, and ExcessHet > 20.

In addition, variants were called using SAMtools mpileup (per scaffold) with the following options: -C50 -pm2 -F0.2 -q 10 -Q 15. Files per scaffold were then converted to VCF format, concatenated (except for the mitochondrial genome), and indexed using BCFtools (v.1.3.1). The VCF file was annotated for ExcessHet and FisherStrand, and the distribution of depth and quality were visually assessed as described above. The VCF file was filtered using the GATK function VariantFiltration with the following values: DP < 1500, DP > 4000, QUAL < 210, FisherStrand > 20, and ExcessHet > 20. Filtered GATK and SAMtools datasets were then combined using bcftools isec. The final VCF file contained variants present in both datasets. Genotypes were then imputed and phased per scaffold using beagle (v.4.0). In total, the final VCF file contained 26,704,097 variants. Chomonomer (v.1.05; http://catchenlab.life.illinois.edu/chromonomer/) was used to place the 3555 *M. zebra* scaffolds in 22 linkage groups using two linkage maps (*57*). For BayPass selection analyses and allele frequency calculations (see below), we excluded indels and nonbiallelic sites, resulting in a VCF file containing 20,343,366 SNPs.

Genetic structure and phylogenetic relationships

Population genetic structure was examined using PCAs implemented in the smartPCA module of Eigensoft (v.6.1.1). To reconstruct a whole-genome nuclear phylogeny, a sequence corresponding to the first haplotype of each scaffold was extracted using bcftools consensus --haplotype 1 of BCFtools v1.5 (https://github.com/samtools/bcftools). Individual whole-genome sequences were then concatenated and a maximum likelihood (ML) analysis was performed in RAxML (v.8.2.11) using the GTRGAMMA sequence evolution model and 20 fast bootstrap replicates. The option *–f a* was used to report the best-scoring ML tree with branch lengths. KBC4, a putative *A. burtoni* individual sampled in the Rusizi River, did not cluster with other *A. burtoni* individuals in the phylogeny (labeled "hybrid"

in fig. S1A). This specimen results most likely from a hybridization event with *Astatoreochromis alluaudi*, as its mitochondrial genome is identical to *A. alluaudi* (fig. S8). Therefore, this individual was excluded from further analyses. To test for introgression or retention of ancestral polymorphism between sympatric species (that is, *A. burtoni* and *H. stappersii* in the Rusizi system and *A. burtoni* and *C. horei* in the Lufubu system), a topology weighting analysis reconstructing fixed-length 5-kb-window phylogenies was performed using Twisst [topology weighting by iterative sampling of subtrees (*58*)].

Demographic modeling

For each of the nine lake-stream population pairs, demographic simulations based on the joint site frequency spectrum (SFS) were performed to estimate the most likely model of population divergence and the best values of demographic parameters (effective population sizes, divergence times, and migration rates). Simulated SFS were obtained using diffusion approximation implemented in ∂a∂I (v.1.7.0) (*59*). A modified version of the program including additional predefined models and the calculation of the Akaike information criterion (AIC) for model selection was used for the simulations (*60*). Eight demographic models of population divergence were tested (fig. S3A): Bottle-Growth (BG), Strict Isolation (SI), Isolation with Migration (IM), Ancient Migration (AM), Secondary Contact (SC), and versions of these models including two categories of migration rates (IM2M, AM2M, and SC2M). These two categories of migration rates can separate, for example, selected versus neutral loci. For the population pairs with a genome-wide $F_{ST} > 0.47$ (*A. burtoni* Lufubu, *C. horei* Lufubu, and *P. philander*), the model BG was not tested, as it was obvious that the populations are separated. Each model was fitted to the observed joint SFS using three successive optimization steps: "hot" simulated annealing, "cold" simulated annealing, and Broyden-Fletcher-Goldfarb-Shanno method (BFGS) (*60*). For each lake-stream population pair, 20 replicates comparing seven or eight models were run using different parameter starting values to ensure convergence. After these 20 runs, the model displaying the lowest AIC and the least variance among the replicates was chosen as the best model. For parameter estimation, additional runs were performed so that the total number of runs was 20 for the best model. To calculate the divergence times in years, a generation time of 1 year was used. As the scaled mutation rate parameter θ was estimated, we used the relation $\theta = 4 \times Ne \times \mu \times L$ to infer the ancestral effective population size (Ne). The mutation rate (μ) (3.51×10^{-9} mutation per generation per year) of Lake Malawi cichlids (*40*) and the length of the genome assembly (L) of *M. zebra* (UMD1: 859,842,111 bp) were applied.

Regions of differentiation

For each lake-stream system, genome-wide F_{ST} (Hudson's estimator of F_{ST}), $|\pi_{lake} - \pi_{stream}|$ (absolute value of the difference in nucleotide diversity between the lake and the river populations), and d_{XY} (absolute divergence) were calculated in 10-kb nonoverlapping sliding windows using evo (https://github.com/millanek/evo). We defined as window of differentiation each window that was contained in the overlap of the top 5% values of these three metrics. Adjacent differentiation windows and windows separated by 10 kb were then merged in differentiation regions. To test whether the differentiation regions of each system are affected by chromosome center–biased differentiation (*30*), each region was placed either in the "center" or in the "periphery" categories. These categories were defined by splitting each chromosome into four parts of equal length, where the center category encompassed the two central parts of the chromosome and the periphery category encompassed the two external parts.

Bayesian selection and association analyses

To detect signatures of selection at the SNP level, we used the Bayesian method BayPass (*31*). The core model performs a genome scan for differentiation by estimating a population covariance matrix of allele frequencies. It allows determining outlier SNPs based on the top 1% of simulated *XtX* values, where *XtX* is a differentiation measure corresponding to an SNP-specific F_{ST} corrected for the scaled covariance of population allele frequencies (*31*). As the northern and southern populations of *A. burtoni* are highly divergent [see (*24*) and fig. S1], only the southern *A. burtoni* populations were analyzed jointly. We thus compared outlier sets for the southern populations of *A. burtoni*, the northern populations of *A. burtoni*, and *H. stappersii*. For the southern *A. burtoni* populations, an additional association analysis using one categorical covariate (lake versus stream) was performed using the auxiliary variable covariate model. Five replicate runs were performed using different starting seed values and default search parameters, except for the number of pilot runs (*25*). The final correlated SNP set contained the overlap of SNPs for which the Bayes factor was higher than 10 and which were in the top 5% of δ values (the posterior probability of association of the SNP with the covariable) in the five replicate runs.

GO annotation and enrichment analyses

To infer whether candidate genes in differentiation regions were enriched for a particular function, all genes included in differentiation regions of each lake-stream system were extracted. In addition, genes including overlapping SNPs between the southern *A. burtoni*, the northern *A. burtoni*, and *H. stappersii* core outliers were reported, as well as genes including overlapping SNPs between *A. burtoni* core outliers and SNPs significantly correlated with lake versus stream environment and morphology. All candidate genes were blasted (blastx) against the NR database (version 12.10.2017) using BLAST+ v.2.6.0, and the first 50 hits were reported. To obtain a reference gene set, all *M. zebra* genes were blasted against NR in the same way. GO and InterProScan annotations were retrieved from Blast2GO PRO (v.4.1.9). Enrichment analyses were performed using Fisher's exact test for each differentiated gene set (one set per system) against the reference gene set (significance level, 0.001). For the genes located in the overlap of differentiation regions among systems, an additional step was performed by manually retrieving the annotations from *Homo sapiens* dataset in UniProt (accessed online 20.11.2017).

Diversification dynamics and genomic divergence in similar versus contrasted environments

To infer the dynamics of genomic differentiation along the lake-stream axis, genome-wide pairwise F_{ST} and the net nucleotide difference D_a [as proxy of time since differentiation; $d_{XY} - (\pi_1 + \pi_2/2)$] were calculated for all possible population pair combinations, resulting in 136 within and between systems comparisons. A logarithmic regression was fitted to the data using the lm function [$\text{lm}(F_{ST}) \sim \ln(D_a)$] implemented in R (v.3.4.2). To estimate the influence of divergent selection at early stages of genomic differentiation in sympatry/parapatry, population pairwise F_{ST} of the southern populations of

A. burtoni were used ("lake-lake," six comparisons; "lake-stream," five comparisons), as well as the pairwise D_M (see below). The northern *A. burtoni* populations were not used because of the high levels of genomic divergence compared to the southern populations. For each comparison, the geographic coastline distance between populations was measured using Google Earth (www.google.com/intl/en/earth/). Then, a linear model was fitted for each category (lake-lake and lake-stream) and the adjusted coefficient of determination R^2 was reported in R.

Morphometric analyses

Geometric morphometrics was used to compare adult body shape between populations. Three juvenile individuals of *P. philander* from Mbulu creek whose genomes had been sequenced were excluded from the morphological analyses. In total, the photographs of 468 individuals (table S2) were used for geometric morphometric analyses (289 *A. burtoni*, 81 *H. stappersii*, 67 *C. horei*, and 31 *P. philander).* Using tpsDig2 (v.2.26), we placed 17 homologous landmarks (fig. S2A) on the lateral image of each fish. The tps file with *x* and *y* coordinates was used as an input for the program MorphoJ (v.1.06d) and superimposed with a Procrustes generalized least squares fit algorithm to remove all nonshape variation (i.e., size, position, and orientation). In addition, the data were corrected for allometric size effects using the residuals of the regression of shape on centroid size for further analyses. CVA and PCA were used to assess shape variation among *A. burtoni* populations (Fig. 3C) and among all populations of the four species (Fig. 3D and fig. S2, B to D). The mean shape distances of CVA were obtained using permutation tests (10,000 permutations). Mahalanobis distances (D_M) among groups from the CVA were calculated and plotted against genetic distances (F_{ST} for within *A. burtoni* comparisons and d_{XY} for between species comparisons).

Vectors of phenotypic and genomic divergence

We followed the method first developed by Adams and Collyer (*32*) and described in detail by Stuart *et al.* (*33*) and Bolnick *et al.* (*13*) to calculate multivariate vectors of phenotypic and genomic divergence. For vectors of morphological divergence, 37 traits and landmarks were used: centroid size (17 landmarks), standard length (landmarks 1 to 14), body depth (landmarks 8 to 12) corrected by standard length (BD/SL ratio), and the *x* and *y* coordinates of each of the 17 landmarks. We then calculated two types of vectors of genomic divergence. First, outlier vectors were calculated using the first 78 PCs (88% variance; same as for non-outliers) of a genomic PCA based on outlier SNPs present in at least one set of BayPass outliers (*H. stappersii* core model, *A. burtoni* North core model, *A. burtoni* South core model, and *A. burtoni* South auxiliary model). Then, "neutral" vectors were calculated using the first 78 PCs of a genomic PCA based on all remaining SNPs (that is, non-outliers) (88% variance; all PC summarizing between-population variation). For each lake-stream pair and, separately, for phenotypic and genomic outlier and non-outlier data, we calculated vector length (L), the difference in length between two vectors (ΔL), and the angle in degrees between two vectors (θ). For each morphological trait (each genomic PC, respectively), we ran *t* tests and used the *t* statistic as an estimate of lake-stream divergence for each trait. Thus, vectors of phenotypic divergence were represented as the matrix $\mathbf{C}_P$ of 37 *t* statistics for each trait/landmark (columns) × 9 lake-stream pairs (rows), and vectors of genomic divergence were represented as a matrix $\mathbf{C}_G$ of 78 *t* statistics for each PC × 9 lake-stream pairs. We calculated nine L_P (phenotype), nine L_G (genotype), nine $L_{G\_outlier}$ values, all lake-stream pairwise comparisons ΔL_P, θ_P, ΔL_G, θ_G, $\Delta L_{G\_outlier}$, and $\theta_{G\_outlier}$. We used Mantel tests (mantel.test function in the ape R package v.5.3; 9999 permutations) to test the correlation between θ_P and $\theta_G/\theta_{G\_outlier}$, ΔL_P and $\Delta L_G/\Delta L_{G\_outlier}$, and linear regression models (lm function in R) to test the correlation between L_P and $L_G/L_{G\_outlier}$.

Multivariate analyses of (non-)parallelism and convergence

In addition to comparing all lake-stream divergence vectors in a pairwise manner, we performed the recently described eigen analyses of vector correlation matrices (**C**) (*34*). These multivariate analyses allow the quantification of the extent of parallelism/antiparallelism by assessing the percentage of variance explained by the leading eigenvectors of **C**. These analyses also reveal how many dimensions of shared evolutionary change exist, by inferring how many eigenvalues are significant. For each dataset (phenotype, genotype outlier, and genotype non-outlier), we calculated the eigen decomposition of the respective matrix of vector correlations **C** described above ($\mathbf{C} = \mathbf{QVQ}^{-1}$) to extract eigenvectors (**Q**) and eigenvalues (**V**) of each dataset. To construct a null expectation of evolutionary parallelism, we used an identity matrix sampled from the *m*-dimensional Wishart distribution with *n* degrees of freedom as suggested by De Lisle and Bolnick (*34*), where *m* is the number of lake-stream pairs and *n* is the number of traits/landmarks. To infer which traits/landmarks/PCs contribute the most to the leading eigenvector of **C**, we investigated the value of trait loadings in the matrix **A**, where $\mathbf{A} = \mathbf{X}^{\mathbf{T}}\mathbf{Q}^{\mathbf{T}-1}$.

Furthermore, we investigated levels of convergence/divergence in multivariate trait space by comparing the among-lineage covariance matrices of trait mean values (**D**) for each environment (*34*). Specifically, for each one of the three datasets (phenotype, genotype outlier, and genotype non-outlier), we calculated $\mathbf{D}_{river}$ and $\mathbf{D}_{lake}$ and their respective trace, which encompasses the total among-lineage variance per environment. To assess levels of convergence/divergence in lake-stream divergence, we then compared both trace values [$\mathrm{tr}(\mathbf{D}_{river}) - \mathrm{tr}(\mathbf{D}_{lake})$], where a negative value indicates convergence (less among-lineage variance in the river environment) and a positive value indicates divergence (more among-lineage variance in the river environment). Last, it has also been proposed to investigate convergence/divergence of a specific trait by estimating the change in Euclidean distance between lineage pairs from different environments (here, river versus lake) (*13*, *34*). We therefore calculated, for each pair of lake-stream systems, the difference in D_M between the respective stream population pair versus lake population pair. For instance, the convergence/divergence in body shape between *A. burtoni* and *C. horei* from the Lufubu system was calculated as follows: (D_M *A.burtoni* Lufubu River – *C.horei* Lufubu River) − (D_M *A.burtoni* Lufubu lake – *C.horei* Lufubu lake), where a negative value indicates convergence and a positive value indicates divergence in body shape.

Predictability of (non-)parallelism

We then investigated the influence of similarity of ancestral (i.e., lake) populations on parallel evolution. We used D_M and F_{ST} between lake populations as proxies of morphological and genetic similarities, respectively. We performed Mantel tests between lake-lake D_M and θ_P and between lake-lake F_{ST} and $\theta_G/\theta_{G\_outlier}$ to infer whether the similarity of ancestral populations between systems was correlated

to the direction of (non-)parallelism. Last, we assessed whether the proportion of standing genetic variation was correlated with the extent of morphological or genetic parallelism. For each of the 136 population pairwise comparison, we extracted allele frequencies of biallelic SNPs using VCFtools --freq command. We then categorized SNPs in four different groups: identical sites (fixed in both populations for the same allele), differentially fixed sites (fixed in both populations for different alleles), fixed and variable sites (fixed in one population and variable in the second population), and standing genetic variation (variable in both populations). We performed Mantel tests between the proportion of standing genetic variation SNPs between lake populations and θ_P and between the proportion of standing genetic variation SNPs and θ_G / $\theta_{G\_outlier}$.

Mate-choice experiments

We used two mate-choice experiments to test for reproductive isolation between the two geographically most distant and genetically most divergent *A. burtoni* populations, Rusizi lake and Kalambo lake (see Supplementary Text and fig. S4). Detailed methods and results of the experiments are provided in Supplementary Text. Briefly, in the first experiment, a two-way female choice setup was used to test whether females preferred males of their own population over others when only visual cues were available (fig. S4A). We placed a gravid female of either population (N = 44) in a central tank and allowed visual contact and interaction with two sized-matched males from Rusizi lake and Kalambo lake presented in two outer tanks. Within a period of up to 12 days, we assessed whether the female had laid the eggs in front of the Rusizi lake male, the Kalambo lake male, in front of both, or in the central section. The position of the laid eggs was used as a measure for female preference (conspecific choice coded as 1 and heterospecific and no choice coded as 0). The binomial data were then analyzed with a generalized linear mixed model, which tested whether the probability of the females spawning with the conspecific male was significantly different from 0.5.

In the second experiment, female spawning decisions were determined in a multisensory setting with free contact between females and males. A single tank was subdivided into three equally sized compartments by plastic grids (fig. S4B). The middle compartment offered a resting and hiding place for the females, whereas the two outer compartments served as male territories. The grid size was chosen to allow the smaller females to migrate between the three compartments and to prevent direct contact between the larger males to exclude male-male competition. We conducted eight trials, each time using two males (one of each population) and six females from both populations (N_{males} = 16; $N_{females}$ = 46). Mouth-brooding females were caught, and 10 larvae from each female were collected for paternity analyses based on five microsatellite markers (*20*). All adult males and females were also genotyped for these five markers. The percentage of fertilized offspring by conspecific or heterospecific males in each replicate was then used to infer whether the females spawned more frequently with the conspecific males. These experiments were performed under the cantonal veterinary permit number 2356.

Statistical analysis

Statistical parameters including the exact value of N are reported in the methods and figure legends. All statistical analyses were performed using R v.3.4.2.

SUPPLEMENTARY MATERIALS

Supplementary material for this article is available at https://science.org/doi/10.1126/sciadv.abg5391

View/request a protocol for this paper from *Bio-protocol*.

REFERENCES AND NOTES

1. C. Darwin, *On the Origins of Species by Means of Natural Selection* (Murray, 1859).
2. J. A. Coyne, H. A. Orr, *Speciation* (Sinauer Associates Inc., 2004).
3. O. Seehausen, R. K. Butlin, I. Keller, C. E. Wagner, J. W. Boughman, P. A. Hohenlohe, C. L. Peichel, G.-P. Saetre, C. Bank, Å. Brännström, A. Brelsford, C. S. Clarkson, F. Eroukhmanoff, J. L. Feder, M. C. Fischer, A. D. Foote, P. Franchini, C. D. Jiggins, F. C. Jones, A. K. Lindholm, K. Lucek, M. E. Maan, D. A. Marques, S. H. Martin, B. Matthews, J. I. Meier, M. Möst, M. W. Nachman, E. Nonaka, D. J. Rennison, J. Schwarzer, E. T. Watson, A. M. Westram, A. Widmer, Genomics and the origin of species. *Nat. Rev. Genet.* **15**, 176–192 (2014).
4. S. Stankowski, M. Ravinet, Defining the speciation continuum. *Evolution* **75**, 1256–1273 (2021).
5. P. Nosil, J. L. Feder, S. M. Flaxman, Z. Gompert, Tipping points in the dynamics of speciation. *Nat. Ecol. Evol.* **1**, 0001 (2017).
6. R. Riesch, M. Muschick, D. Lindtke, R. Villoutreix, A. A. Comeault, T. E. Farkas, K. Lucek, E. Hellen, V. Soria-Carrasco, S. R. Dennis, C. F. de Carvalho, R. J. Safran, C. P. Sandoval, J. Feder, R. Gries, B. J. Crespi, G. Gries, Z. Gompert, P. Nosil, Transitions between phases of genomic differentiation during stick-insect speciation. *Nat. Ecol. Evol.* **1**, 0082 (2017).
7. S. Stankowski, A. M. Westram, Z. B. Zagrodzka, I. Eyres, T. Broquet, K. Johannesson, R. K. Butlin, The evolution of strong reproductive isolation between sympatric intertidal snails. *Philos. Trans. R. Soc. B Biol. Sci.* **375**, 20190545 (2020).
8. Y. Y. Yamasaki, R. Kakioka, H. Takahashi, A. Toyoda, A. J. Nagano, Y. Machida, P. R. Møller, J. Kitano, Genome-wide patterns of divergence and introgression after secondary contact between *Pungitius* sticklebacks. *Philos. Trans. R. Soc. B. Biol. Sci.* **375**, 20190548 (2020).
9. A. T. Sendell-Price, K. C. Ruegg, E. C. Anderson, C. S. Quilodrán, B. M. Van Doren, V. L. Underwood, T. Coulson, S. M. Clegg, The genomic landscape of divergence across the speciation continuum in island-colonising silvereyes (*Zosterops lateralis*). *G3* **10**, 3147–3163 (2020).
10. D. Schluter, L. M. Nagel, Parallel speciation by natural selection. *Am. Nat.* **146**, 292–301 (1995).
11. Z. D. Blount, R. E. Lenski, J. B. Losos, Contingency and determinism in evolution: Replaying life's tape. *Science* **362**, eaam5979 (2018).
12. K. B. Oke, G. Rolshausen, C. LeBlond, A. P. Hendry, How parallel is parallel evolution? A comparative analysis in fishes. *Am. Nat.* **190**, 1–16 (2017).
13. D. I. Bolnick, R. D. Barrett, K. B. Oke, D. J. Rennison, Y. E. Stuart, (Non) parallel evolution. *Annu. Rev. Ecol. Evol. Syst.* **49**, 303–330 (2018).
14. B. Fang, P. Kemppainen, P. Momigliano, X. Feng, J. Merilä, On the causes of geographically heterogeneous parallel evolution in sticklebacks. *Nat. Ecol. Evol.* **4**, 1105–1115 (2020).
15. I. S. Magalhaes, J. R. Whiting, D. D'Agostino, P. A. Hohenlohe, M. Mahmud, M. A. Bell, S. Skúlason, A. D. MacColl, Intercontinental genomic parallelism in multiple three-spined stickleback adaptive radiations. *Nat. Ecol. Evol.* **5**, 251–261 (2021).
16. T. D. Kocher, Adaptive evolution and explosive speciation: The cichlid fish model. *Nat. Rev. Genet.* **5**, 288–298 (2004).
17. W. Salzburger, Understanding explosive diversification through cichlid fish genomics. *Nat. Rev. Genet.* **19**, 705–717 (2018).
18. F. Ronco, M. Matschiner, A. Böhne, A. Boila, H. H. Büscher, A. El Taher, A. Indermaur, M. Malinsky, V. Ricci, A. Kahmen, S. Jentoft, W. Salzburger, Drivers and dynamics of a massive adaptive radiation in cichlid fishes. *Nature* **589**, 76–81 (2021).
19. D. Brawand, C. E. Wagner, Y. I. Li, M. Malinsky, I. Keller, S. Fan, O. Simakov, A. Y. Ng, Z. W. Lim, E. Bezault, J. Turner-Maier, J. Johnson, R. Alcazar, H. J. Noh, P. Russell, B. Aken, J. Alföldi, C. Amemiya, N. Azzouzi, J.-F. Baroiller, F. Barloy-Hubler, A. Berlin, R. Bloomquist, K. L. Carleton, M. A. Conte, H. D'Cotta, O. Eshel, L. Gaffney, F. Galibert, H. F. Gante, S. Gnerre, L. Greuter, R. Guyon, N. S. Haddad, W. Haerty, R. M. Harris, H. A. Hofmann, T. Hourlier, G. Hulata, D. B. Jaffe, M. Lara, A. P. Lee, I. MacCallum, S. Mwaiko, M. Nikaido, H. Nishihara, C. Ozouf-Costaz, D. J. Penman, D. Przybylski, M. Rakotomanga, S. C. P. Renn, F. J. Ribeiro, M. Ron, W. Salzburger, L. Sanchez-Pulido, M. E. Santos, S. Searle, T. Sharpe, R. Swofford, F. J. Tan, L. Williams, S. Young, S. Yin, N. Okada, T. D. Kocher, E. A. Miska, E. S. Lander, B. Venkatesh, R. D. Fernald, A. Meyer, C. P. Ponting, J. T. Streelman, K. Lindblad-Toh, O. Seehausen, F. Di Palma, The genomic substrate for adaptive radiation in African cichlid fish. *Nature* **513**, 375–381 (2014).
20. A. Theis, F. Ronco, A. Indermaur, W. Salzburger, B. Egger, Adaptive divergence between lake and stream populations of an East African cichlid fish. *Mol. Ecol.* **23**, 5304–5322 (2014).
21. C. Sturmbauer, S. Baric, W. Salzburger, L. Rüber, E. Verheyen, Lake level fluctuations synchronize genetic divergences of cichlid fishes in African lakes. *Mol. Biol. Evol.* **18**, 144–154 (2001).

22. W. Salzburger, B. Van Bocxlaer, A. S. Cohen, Ecology and evolution of the African Great Lakes and their faunas. *Annu. Rev. Ecol. Evol. Syst.* **45**, 519–545 (2014).
23. B. Egger, M. Roesti, A. Böhne, O. Roth, W. Salzburger, Demography and genome divergence of lake and stream populations of an East African cichlid fish. *Mol. Ecol.* **26**, 5016–5030 (2017).
24. G. Pauquet, W. Salzburger, B. Egger, The puzzling phylogeography of the haplochromine cichlid fish *Astatotilapia burtoni*. *Ecol. Evol.* **8**, 5637–5648 (2018).
25. F. Ronco, H. H. Büscher, A. Indermaur, W. Salzburger, The taxonomic diversity of the cichlid fish fauna of ancient Lake Tanganyika, East Africa. *J. Great Lakes Res.* **46**, 1067–1078 (2020).
26. A. Böhne, A. A.-T. Weber, J. Rajkov, M. Rechsteiner, A. Riss, B. Egger, W. Salzburger, Repeated evolution versus common ancestry: Sex chromosome evolution in the haplochromine cichlid *Pseudocrenilabrus philander*. *Genome Biol. Evol.* **11**, 439–458 (2019).
27. J. Rajkov, A. A.-T. Weber, W. Salzburger, B. Egger, Adaptive phenotypic plasticity contributes to divergence between lake and river populations of an East African cichlid fish. *Ecol. Evol.* **8**, 7323–7333 (2018).
28. J. Rajkov, A. A.-T. Weber, W. Salzburger, B. Egger, Immigrant and extrinsic hybrid inviability contribute to reproductive isolation between lake and river cichlid ecotypes. *Evolution* **72**, 2553–2564 (2018).
29. J. N. Weber, G. S. Bradburd, Y. E. Stuart, W. E. Stutz, D. I. Bolnick, Partitioning the effects of isolation by distance, environment, and physical barriers on genomic divergence between parapatric threespine stickleback. *Evolution* **71**, 342–356 (2017).
30. D. Berner, M. Roesti, Genomics of adaptive divergence with chromosome-scale heterogeneity in crossover rate. *Mol. Ecol.* **26**, 6351–6369 (2017).
31. M. Gautier, Genome-wide scan for adaptive divergence and association with population-specific covariates. *Genetics* **201**, 1555–1579 (2015).
32. D. C. Adams, M. L. Collyer, A general framework for the analysis of phenotypic trajectories in evolutionary studies. *Evolution* **63**, 1143–1154 (2009).
33. Y. E. Stuart, T. Veen, J. N. Weber, D. Hanson, M. Ravinet, B. K. Lohman, C. J. Thompson, T. Tasneem, A. Doggett, R. Izen, N. Ahmed, R. D. H. Barrett, A. P. Hendry, C. L. Peichel, D. I. Bolnick, Contrasting effects of environment and genetics generate a continuum of parallel evolution. *Nat. Ecol. Evol.* **1**, 0158 (2017).
34. S. P. De Lisle, D. I. Bolnick, A multivariate view of parallel evolution. *Evolution* **74**, 1466–1481 (2020).
35. C. P. Klingenberg, Evolution and development of shape: Integrating quantitative approaches. *Nat. Rev. Genet.* **11**, 623–635 (2010).
36. M.-D. C. de Caprona, Olfactory communication in a cichlid fish, *Haplochromis burtoni*. *Z. Tierpsychol.* **52**, 113–134 (1980).
37. J. A. Coyne, H. A. Orr, Patterns of speciation in Drosophila. *Evolution* **43**, 362–381 (1989).
38. J. M. Coughlan, D. R. Matute, The importance of intrinsic postzygotic barriers throughout the speciation process. *Philos. Trans. R. Soc. B Biol. Sci.* **375**, 20190533 (2020).
39. C. Roux, C. Fraisse, J. Romiguier, Y. Anciaux, N. Galtier, N. Bierne, Shedding light on the grey zone of speciation along a continuum of genomic divergence. *PLOS Biol.* **14**, e2000234 (2016).
40. M. Malinsky, H. Svardal, A. M. Tyers, E. A. Miska, M. J. Genner, G. F. Turner, R. Durbin, Whole-genome sequences of Malawi cichlids reveal multiple radiations interconnected by gene flow. *Nat. Ecol. Evol.* **2**, 1940–1955 (2018).
41. J. I. Meier, D. A. Marques, C. E. Wagner, L. Excoffier, O. Seehausen, Genomics of parallel ecological speciation in Lake Victoria cichlids. *Mol. Biol. Evol.* **35**, 1489–1506 (2018).
42. E. Verheyen, L. Rüber, J. Snoeks, A. Meyer, Mitochondrial phylogeography of rock-dwelling cichlid fishes reveals evolutionary influence of historical lake level fluctuations of Lake Tanganyika, Africa. *Philos. Trans. R. Soc. Lond. B Biol. Sci.* **351**, 797–805 (1996).
43. M. Malinsky, R. J. Challis, A. M. Tyers, S. Schiffels, Y. Terai, B. P. Ngatunga, E. A. Miska, R. Durbin, M. J. Genner, G. F. Turner, Genomic islands of speciation separate cichlid ecomorphs in an East African crater lake. *Science* **350**, 1493–1498 (2015).
44. M. Ravinet, R. Faria, R. K. Butlin, J. Galindo, N. Bierne, M. Rafajlović, M. A. F. Noor, B. Mehlig, A. M. Westram, Interpreting the genomic landscape of speciation: A road map for finding barriers to gene flow. *J. Evol. Biol.* **30**, 1450–1477 (2017).
45. R. Burri, Interpreting differentiation landscapes in the light of long-term linked selection. *Evolution Lett.* **1**, 118–131 (2017).
46. J. Rajkov, A. E. Taher, A. Böhne, W. Salzburger, B. Egger, Gene expression remodelling and immune response during adaptive divergence in an African cichlid fish. *Mol. Ecol.* **30**, 274–296 (2021).
47. A. V. Artemov, N. S. Mugue, S. M. Rastorguev, S. Zhenilo, A. M. Mazur, S. V. Tsygankova, E. S. Boulygina, D. Kaplun, A. V. Nedoluzhko, Y. A. Medvedeva, E. B. Prokhortchouk, Genome-wide DNA methylation profiling reveals epigenetic adaptation of stickleback to marine and freshwater conditions. *Mol. Biol. Evol.* **34**, 2203–2213 (2017).
48. Y. Hu, R. C. Albertson, Baby fish working out: An epigenetic source of adaptive variation in the cichlid jaw. *Proc. R. Soc. B Biol. Sci.* **284**, 20171018 (2017).
49. J. F. Storz, Causes of molecular convergence and parallelism in protein evolution. *Nat. Rev. Genet.* **17**, 239–250 (2016).
50. F. C. Jones, M. G. Grabherr, Y. F. Chan, P. Russell, E. Mauceli, J. Johnson, R. Swofford, M. Pirun, M. C. Zody, S. White, E. Birney, S. Searle, J. Schmutz, J. Grimwood, M. C. Dickson, R. M. Myers, C. T. Miller, B. R. Summers, A. K. Knecht, S. D. Brady, H. Zhang, A. A. Pollen, T. Howes, C. Amemiya; Broad Institute Genome Sequencing Platform, W. G. A. Team, E. S. Lander, F. D. Palma, K. Lindblad-Toh, D. M. Kingsley, The genomic basis of adaptive evolution in threespine sticklebacks. *Nature* **484**, 55–61 (2012).
51. K. A. Thompson, M. M. Osmond, D. Schluter, Parallel genetic evolution and speciation from standing variation. *Evol. Lett.* **3**, 129–141 (2019).
52. A. Paccard, D. Hanson, Y. E. Stuart, F. A. von Hippel, M. Kalbe, T. Klepaker, S. Skúlason, B. K. Kristjánsson, D. I. Bolnick, A. P. Hendry, R. D. H. Barrett, Repeatability of adaptive radiation depends on spatial scale: Regional versus global replicates of stickleback in lake versus stream habitats. *J. Hered.* **111**, 43–56 (2020).
53. C. P. Klingenberg, M. Barluenga, A. Meyer, Body shape variation in cichlid fishes of the *Amphilophus citrinellus* species complex. *Biol. J. Linn. Soc.* **80**, 397–408 (2003).
54. P. Franchini, C. Fruciano, M. L. Spreitzer, J. C. Jones, K. R. Elmer, F. Henning, A. Meyer, Genomic architecture of ecologically divergent body shape in a pair of sympatric crater lake cichlid fishes. *Mol. Ecol.* **23**, 1828–1845 (2014).
55. A. F. Kautt, C. F. Kratochwil, A. Nater, G. Machado-Schiaffino, M. Olave, F. Henning, J. Torres-Dowdall, A. Härer, C. D. Hulsey, P. Franchini, M. Pippel, E. W. Myers, A. Meyer, Contrasting signatures of genomic divergence during sympatric speciation. *Nature* **588**, 106–111 (2020).
56. M. O. B. Reiskind, M. L. Moody, D. I. Bolnick, C. T. Hanifin, C. E. Farrior, Nothing in evolution makes sense except in the light of biology. *Bioscience* **71**, 370–382 (2021).
57. C. T. O'Quin, A. C. Drilea, M. A. Conte, T. D. Kocher, Mapping of pigmentation QTL on an anchored genome assembly of the cichlid fish, *Metriaclima zebra*. *BMC Genomics* **14**, 287 (2013).
58. S. H. Martin, S. M. Van Belleghem, Exploring evolutionary relationships across the genome using topology weighting. *Genetics* **206**, 429–438 (2017).
59. R. N. Gutenkunst, R. D. Hernandez, S. H. Williamson, C. D. Bustamante, Inferring the joint demographic history of multiple populations from multidimensional SNP frequency data. *PLOS Genet.* **5**, e1000695 (2009).
60. M. Tine, H. Kuhl, P.-A. Gagnaire, B. Louro, E. Desmarais, R. S. Martins, J. Hecht, F. Knaust, K. Belkhir, S. Klages, R. Dieterich, K. Stueber, F. Piferrer, B. Guinand, N. Bierne, F. A. M. Volckaert, L. Bargelloni, D. M. Power, F. Bonhomme, A. V. M. Canario, R. Reinhardt, European sea bass genome and its variation provide insights into adaptation to euryhalinity and speciation. *Nat. Commun.* **5**, 5770 (2014).
61. A. Theis, W. Salzburger, B. Egger, The function of anal fin egg-spots in the cichlid fish *Astatotilapia burtoni*. *PLOS ONE* **7**, e29878 (2012).
62. A. Theis, T. Bosia, T. Roth, W. Salzburger, B. Egger, Egg-spot pattern and body size asymmetries influence male aggression in haplochromine cichlid fishes. *Behav. Ecol.* **26**, 1512–1519 (2015).
63. G. P. Baerends, J. M. Baerends-Van Roon, in *An Introduction to the Study of the Ethology of the Cichlid Fishes* (Brill, 1950), pp. 1–243.
64. P. D. Dijkstra, S. M. Maguire, R. M. Harris, A. A. Rodriguez, R. S. DeAngelis, S. A. Flores, H. A. Hofmann, The melanocortin system regulates body pigmentation and social behaviour in a colour polymorphic cichlid fish†. *Proc. R. Soc. B Biol. Sci.* **284**, 20162838 (2017).
65. K. P. Maruska, U. S. Ung, R. D. Fernald, The African cichlid fish *Astatotilapia burtoni* uses acoustic communication for reproduction: Sound production, hearing, and behavioral significance. *PLOS ONE* **7**, e37612 (2012).
66. D. Bates, M. Maechler, B. Bolker, S. Walker, lme4: Linear mixed-effects models using Eigen and S4. R package version 1.1–7 (2015).
67. R Core Team, *R: A Language and Environment for Statistical Computing* (R Foundation for Statistical Computing, 2017).
68. M. Plenderleith, C. Van Oosterhout, R. L. Robinson, G. F. Turner, Female preference for conspecific males based on olfactory cues in a Lake Malawi cichlid fish. *Biol. Lett.* **1**, 411–414 (2005).
69. M. I. Taylor, F. Meardon, G. Turner, O. Seehausen, H. D. Mrosso, C. Rico, Characterization of tetranucleotide microsatellite loci in a Lake Victorian, haplochromine cichlid fish: A *Pundamilia pundamilia* x *Pundamilia nyererei* hybrid. *Mol. Ecol.* **2**, 443–445 (2002).
70. W.-J. Lee, T. D. Kocher, Microsatellite DNA markers for genetic mapping in *Oreochromis niloticus*. *J. Fish Biol.* **49**, 169–171 (1996).
71. M. Sanetra, F. Henning, S. Fukamachi, A. Meyer, A microsatellite-based genetic linkage map of the cichlid fish, *Astatotilapia burtoni* (Teleostei): A comparison of genomic architectures among rapidly speciating cichlids. *Genetics* **182**, 387–397 (2009).
72. S. T. Kalinowski, M. L. Taper, T. C. Marshall, Revising how the computer program CERVUS accommodates genotyping error increases success in paternity assignment. *Mol. Ecol.* **16**, 1099–1106 (2007).

Acknowledgments: We would like to thank F. Ronco, A. Indermaur, and G. Pauquet for help during fieldwork; the crews of the Kalambo Lodge and the Ndole Bay Lodge for logistic support in Zambia; and the Lake Tanganyika Research Unit, Department of Fisheries, Republic of Zambia and the University of Burundi, the Ministère de l'Eau, de l'Environnement, de l'Amenagement du Territoire et de l'Urbanisme, Republic of Burundi for research permits. We thank A. El Taher and M. Malinsky for help with data analyses; M. Conte for sharing the Chromonomer results; A. Böhne, M. Matschiner, and four anonymous reviewers for valuable comments on the manuscript; and J. Johnson for fish illustrations. Last, we are grateful to the support team of sciCORE (Center for Scientific Computing, University of Basel; http://scicore.unibas.ch/), especially P. E. Lopez. **Funding:** This study was supported by grants from the Swiss Zoological Society (SZS) to J.R. and the Swiss National Science Foundation (SNSF; grants 31003A_156405 and 3100A_176039) to W.S. A.A.-T.W. is currently supported by an Endeavour Postdoctoral Fellowship awarded by the Australian Department of Education and Training (grant agreement 6534_2018) and a Marie Skłodowska-Curie Global Fellowship awarded by the Research Executive Agency of the European Commission (grant agreement 797326).

Author contributions: B.E. and W.S. conceived and supervised the study. All coauthors conducted the fieldwork. A.A.-T.W. and J.R. conducted the molecular laboratory work. J.R. generated and analyzed the morphometric data. K.S. and B.E. designed, conducted, and analyzed the mate-choice experiments. A.A.-T.W. analyzed the genomic data. A.A.-T.W. and W.S. drafted the manuscript, with feedback from all coauthors. **Competing interests:** The authors declare that they have no competing interests. **Data and materials availability:** The raw sequence reads were deposited on SRA and are available with accession numbers SRP156808 (*A. burtoni*, *C. horei*, and *H. stappersii*) and SRP148476 (*P. philander*). All data needed to evaluate the conclusions in the paper are present in the paper and/or the Supplementary Materials.

Submitted 12 January 2021
Accepted 14 September 2021
Published 3 November 2021
10.1126/sciadv.abg5391

ScienceAdvances

Speciation dynamics and extent of parallel evolution along a lake-stream environmental contrast in African cichlid fishes

Alexandra A.-T. WeberJelena RajkovKolja SmailusBernd EggerWalter Salzburger

Sci. Adv., 7 (45), eabg5391.